Structure of Terephthalate Polymers I—Infra-red Spectra and Molecular Structure of Poly(ethylene terephthalate)

T. R. MANLEY and D. A. WILLIAMS

The 'rigid' crystalline model for poly(ethylene terephthalate) is not wholly consistent with the infra-red spectra of PET and model compounds, including polarized spectra in the far infra-red (600–20 cm^{-1}). The results indicate that the extent of rotation of the glycol fragment about the terephthalate framework in the PET crystal appears to be greater than in the above model. The space group $P\bar{1}$ is, however, conserved. There appears to be more rotational hindrance in the crystal than in the amorphous polymer about the —CH_2—O— *and* —C—O— *bonds and the existence of the discrete* trans *and* gauche *glycol configurations has been confirmed. The degree of crystallinity of PET is correlated with the* trans *glycol residue and a planar terephthalate framework. Conversely the amorphous content is correlated with the* gauche *form of the glycol residue and an accompanying distortion of the terephthalate framework from V_h to C_{2v} symmetry. Assignments for the vibrational modes of the terephthalate framework have been made on the basis of V_h and C_{2v} symmetries for the* trans *and* gauche *isomers in PET, respectively, using information from the related poly(cyclohexane-1,4-dimethylene terephthalate). The assignments of the vibrational modes for the ethylene glycol fragment on the basis of C_{2h} symmetry* (trans *isomer) and C_2 symmetry* (gauche *isomer) are also given together with assignments for the principal stretching, deformation and torsional modes of the backbone chain for each configuration. These are found to be in reasonable agreement with calculated values.*

THE spectral change accompanying the drawing of poly(ethylene terephthalate) (PET) has been attributed[1-4] almost entirely to *trans–gauche* rotational isomerism of the ethylene glycol residue, —OCH_2CH_2O—. Most workers assume that the intensity variations of many of the bands in PET upon crystallization are due to the change from the predominantly *trans* configuration of the highly crystalline material to the predominantly *gauche* configuration of the amorphous polymer. However, the related polymer *trans*-poly(cyclohexane-1,4-dimethylene terephthalate) (PCHT) which does not possess the glycol residue, contains bands common to PET which change in intensity upon crystallization. It seems unlikely that rotational isomerism of the glycol residue is wholly responsible for these changes in PET. The terephthalate framework, which is common to PET and PCHT, contributes most of the absorption bands of direct crystal or amorphous origin. This is attributed to the departure of the framework from planarity in the amorphous regions of the polymer as otherwise these bands would be expected to remain unaffected by the amorphous to crystalline transition.

Previous studies on PET in the infra-red[5-7] have attempted to elucidate the changes occurring in the conventional region of the spectrum as a result of deuteration and crystallization, and only partial assignments of the vibrational spectrum of the polymer repeat unit have been attempted[5,6]. In this

investigation a more thorough assignment of the repeat unit has been made with the aid of the polarized far infra-red measurements, and the skeletal deformation and torsional modes have been assigned. This has in turn enabled a more complete interpretation to be made of the change in spectral behaviour of the polymer upon orientation and crystallization. In order to assist in making assignments, various model compounds have been examined throughout the infra-red region. The following types of PET were examined as thin films: (1) amorphous, (2) uniaxially oriented and heat treated, (3) uniaxially oriented but not heat treated, (4) doubly oriented and heat treated, and (5) doubly oriented but not heat treated. The instruments used were: (*i*) Grubb Parsons double-beam prism and grating spectrometers 'GS-3' and 'Spectromaster' (5 000–500 cm^{-1}), (*ii*) Grubb Parsons 'DM-4' far infra-red double-beam grating spectrometer (500–200 cm^{-1}), and (*iii*) Grubb Parsons–NPL interferometric spectrometers (single-beam) of both 3 in. and 5 in. diameter optics (400–20 cm^{-1}).

The oriented films 20–100 μm thick, were examined between 5 000–500 cm^{-1} with polarized radiation produced from a silver chloride pile-of-plate transmission polarizer, consisting of six AgCl sheets (thickness 0·010 in.) set at the Brewster angle of 64°. Polarized far infra-red radiation (500–20 cm^{-1}) was produced from a pile-of-plate polyethylene transmission polarizer. In order to compensate for the appreciably polarized radiation produced from each instrument, the principal stretching axis of each sample, having been detected with the aid of an optical polarizing microscope, was aligned and fixed at 45° to the spectrometer slit. The polarizer was then rotated so that the electric vector of the radiation incident on the film was in turn parallel and perpendicular to the axis of orientation of the film sample. Since the films could not readily be studied in projections parallel to the plane of the sheets the orientation studies were confined to only two of the three principal axes, namely the axis of stretching and the axis perpendicular to the orientation axis in the plane of the film. Studies of the far infra-red absorption about the axis mutually perpendicular to the principal stretching axis and the plane of the film using both the tilting method and the microspectroscopic technique have not yet been carried out due to experimental difficulties. Tadokoro *et al.*[8] have used the latter techniques to examine the dichroism of drawn PET in the conventional infra-red.

Selected far infra-red transmission filters[9] and beam splitters of doubly oriented PET of various thicknesses were employed in the interferometers to enable the entire frequency range of interest (400–20 cm^{-1}) to be examined to the best advantage. The spectra were computed from the interferograms (IBM 1120). The resulting spectra were accurate to within one per cent transmittance and the errors in the frequency were less than 2 cm^{-1}, but some of the far infra-red bands are so broad that the uncertainty in choosing the origin is several times this amount.

In all the PET samples examined the effects of drawing and heat treatment were most apparent in the far infra-red spectral region, resulting in significant shifts in frequency and changes in intensity in many of the bands. The results of the far infra-red studies are summarized in *Table 5*. The corresponding conventional infra-red spectra show far fewer changes

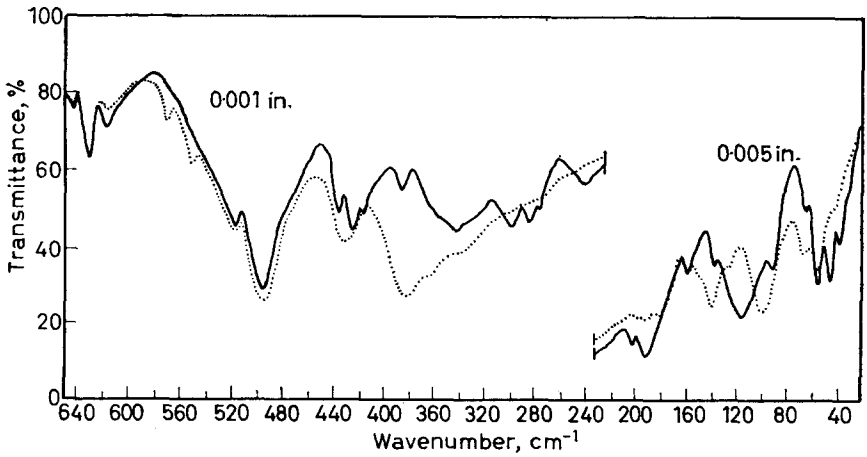

Figure 1—Effect of drawing and heat treatment on the far infra-red spectrum of amorphous PET (..... 1-way drawn; —— amorphous)

and the results are summarized in *Table 6*. *Figure 1* shows the far infra-red spectra of amorphous PET and of amorphous PET which has been subsequently drawn in one direction and annealed at 180°C.

Figure 2 shows the changes produced in the far infra-red spectrum of amorphous PET film due to cold drawing alone and *Figure 3* shows the effect of subsequent heat treatment at 180°C on the far infra-red spectrum of this cold drawn PET film. *Figure 4* illustrates the pronounced changes which occur in the infra-red spectrum of the one-way drawn heat-treated film upon biaxial (plane) orientation and *Figure 5* shows the effect of

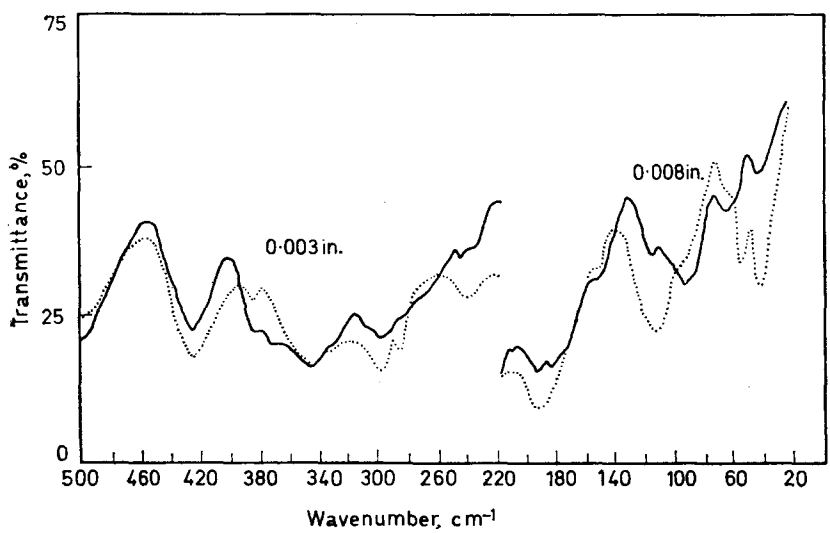

Figure 2—Effect of cold drawing on the far infra-red spectrum of amorphous PET (..... amorphous; —— 1-way drawn)

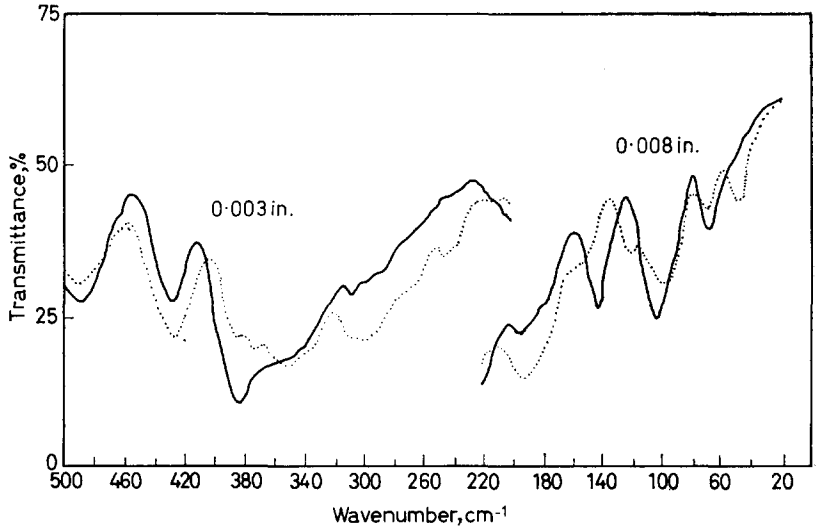

Figure 3—Effect of heat treatment on the far infra-red spectrum of uniaxially oriented (cold drawn) PET
(..... uniaxially oriented, cold drawn; —— heat treated)

annealing a biaxially oriented (cold drawn) PET film on the far infra-red spectrum. The polarized far infra-red spectra of uniaxially oriented (cold drawn) and heat-treated PET have been published elsewhere[10].

MODEL COMPOUNDS

The model compounds studied as an aid to the structural analysis of PET

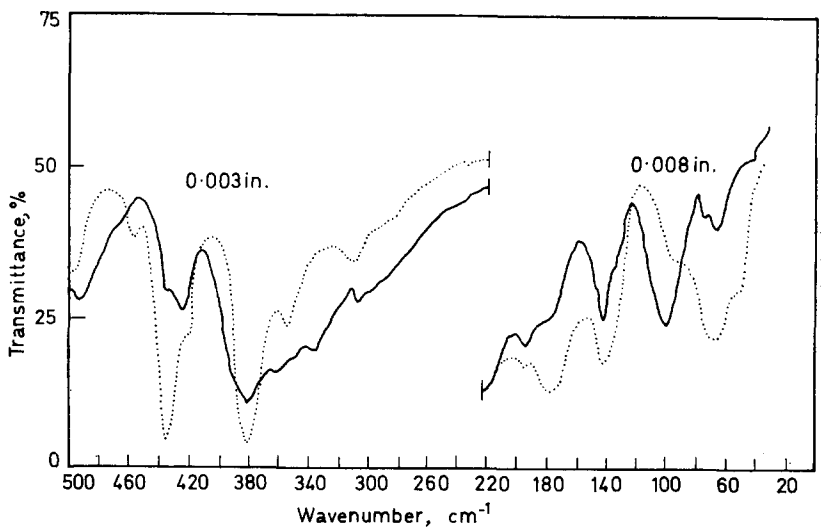

Figure 4—Far infra-red spectra of heat-treated uniaxially and biaxially oriented PET
(—— 1-way drawn; ..... 2-way drawn)

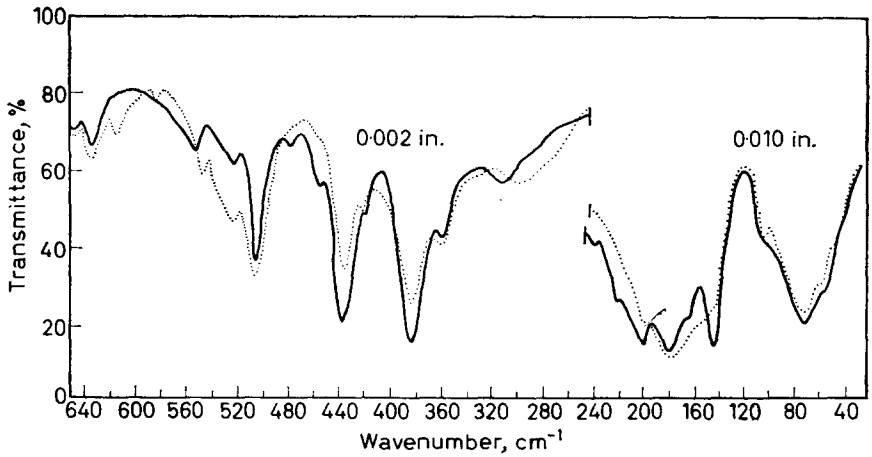

Figure 5—Effect of heat treatment on the far infra-red spectrum of biaxially oriented (cold drawn) PET (..... cold drawn; —— heat treated)

included terephthalic acid, ethylene glycol, ethylene glycol dibenzoate, 1,6-hexanediol dibenzoate,

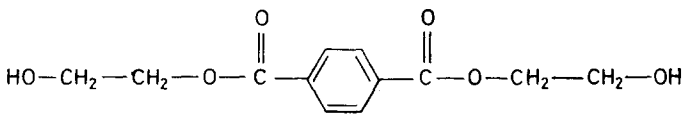

bis-β-hydroxyethyl terephthalate, and

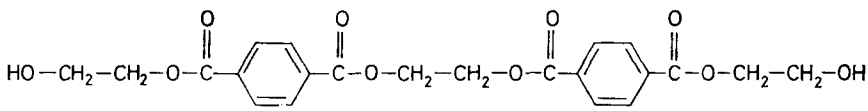

ethylene glycol terephthalate 'oligomer'.

Samples of the model compounds obtained under various conditions of crystallization and in solution in suitable solvents were examined in the region 5 000–500 cm^{-1} in potassium bromide and, where possible, as crystalline deposits on a potassium bromide window. In the far infra-red the compounds were investigated as finely ground dispersions in 'Rigidex' polyethylene discs, as Nujol mulls and as crystalline deposits on polyethylene substrates. The infra-red spectra of some of these compounds in the solid state were found to vary according to the conditions of crystallization. The spectra of the compounds in solution are virtually the same as those of the molten state[4]. The infra-red spectrum of amorphous PET film is very similar to the spectrum of the molten polymer[8].

The infra-red spectra and band assignments of the model compounds for PET are summarized in *Table 7*.

PREDICTED SPECTRUM OF POLY(ETHYLENE TEREPHTHALATE)

Before any vibrational assignments of the polymer can be attempted it is necessary to predict the number of normal modes of vibration and their associated activity in the polymer repeat unit

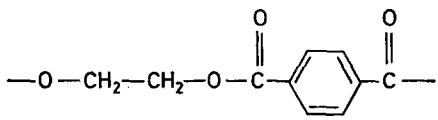

for a specific configuration. To achieve this the local symmetries of portions of the repeat unit must be considered. On the basis of the results of Bunn *et al.*[11], for the structure of crystalline PET, the factor group or unit cell group is isomorphic with the point group C_i. Consideration of the unit cell on the basis of C_i symmetry is not helpful in interpreting the spectrum of PET[5]. However, if the two fragments

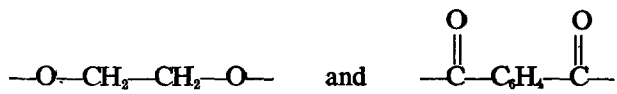

which make up the unit cell are considered separately, the results are much more informative. This approximate method for treating the spectra of high polymers has been applied successfully to a number of polymers[12,13].

THE NORMAL MODES OF VIBRATION OF THE FRAGMENT —C(=O)—C$_6$H$_4$—C(=O)—

The terephthalate fragment —C(=O)—C$_6$H$_4$—C(=O)— is expected to have $(3N-6)$, i.e. $(42-6)$, normal modes of vibration. Of these 36 fundamentals, 24 are skeletal modes involving essentially vibrations of the —C(=O)—C$_6$—C(=O)— framework, and the 12 remaining modes are due to motions of the hydrogen atoms moving with respect to an essentially rigid —C(=O)—C$_6$—C(=O)— framework. Of the 24 skeletal modes, six will be due to the motion of the oxygen atoms moving with respect to a rigid —C—C$_6$H$_4$—C— framework, involving essentially the stretching of the C=O bond, $\nu_{C=O}$ (two modes due to in-phase and out-of-phase C=O stretching), and parallel and perpendicular motion of the oxygen atoms with respect to the plane of the benzene ring. (There will be two parallel C=O deformation modes, $\omega_{C=O}$ (C=O wagging), and two perpendicular C=O deformation modes, $\rho_{C=O}$ (C=O rocking modes), respectively. The remaining 18 skeletal modes will consist

of internal motions of the —C(=O)—C_6—C(=O)— framework, in which the C=O groups move as a unit.

If it is assumed that the —C(=O)—C_6H_4—C(=O)— framework is planar, and that it has a centre of symmetry as the X-ray diffraction analysis[11] suggests, then the fragment will possess V_h (i.e. D_{2h}) symmetry. In this case the axis through the para substituents is taken as the y axis, and the axis perpendicular to the plane of the benzene ring as the z axis. All 36 modes transform according to the characters of the eight irreducible representations for V_h symmetry, summarized in *Table 1*. These 36 normal modes are then found to divide as follows:

$$7A_g + 6B_{1g} + 1B_{2g} + 4B_{3g} + 2A_u + 4B_{1u} + 6B_{2u} + 6B_{3u}$$

in which the A_g, B_{1g}, B_{2g} and B_{3g} modes are only active in the Raman effect. The A_u modes are inactive in both effects. The B_{1u}, B_{2u} and B_{3u} modes are active only in the infra-red. The numbering and description of the approximate motions of the 36 normal modes under V_h symmetry are given in *Table 9*.

As already stated, the X-ray diffraction analysis[11] indicated a slight departure from planarity of the [—C(=O)—C_6H_4—C(=O)—] framework. The most

likely symmetry of the non-planar terephthalate framework will be C_{2v}, in which the single twofold rotation axis of the fragment will be the z axis which is perpendicular to the plane of the benzene ring. On reduction to C_{2v} symmetry from the V_h configuration, which involves the loss of the two twofold rotation axes $C_2(x)$ and $C_2(y)$ and the $\sigma(xy)$ plane due to non-planarity, the 36 normal modes of the terephthalate framework, according to the characters for C_{2v} symmetry given in *Table 2*, divide as follows:

$$11A_1 + 8A_2 + 7B_1 + 10B_2$$

where the A_1, B_1 and B_2 species are active in both the Raman and infra-red effects, the A_2 species being active only in the Raman. The correlations between the corresponding modes of the V_h and C_{2v} symmetry species are given in *Tables 2* and *9*. It is to be noted that on the basis of V_h symmetry for a planar terephthalate framework, only 16 of the 36 fundamental modes will be infra-red active. In C_{2v} symmetry, however, 28 of the 36 normal modes will be active in the infra-red. Since the departure from planarity is known to be only slight in highly crystalline PET, the A_g, B_{2g} and B_{3g} species, which are the infra-red inactive modes of V_h symmetry, and which become the infra-red active A_1, B_1 and B_2 modes of C_{2v} symmetry (*Table 9*), are expected to occur as extremely weak bands in the infra-red spectrum of highly oriented, crystalline specimens of PET.

Table 1. Characters and selection rules for the fragment 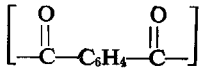 in PET on the basis of V_h symmetry

$V_h \equiv D_{2h}$	E	$C_2(z)$	$C_2(y)$	$C_2(x)$	i	$\sigma(xy)$	$\sigma(zx)$	$\sigma(yz)$	n		
A_g	1	1	1	1	1	1	1	1	7		$\alpha_{xx}, \alpha_{uu}, \alpha_{zz}$
B_{1g}	1	1	−1	−1	1	1	−1	−1	6	R_z	α_{xu}
B_{2g}	1	−1	1	−1	1	−1	1	−1	1	R_u	α_{zx}
B_{3g}	1	−1	−1	1	1	−1	−1	1	4	R_x	α_{uz}
A_u	1	1	1	1	−1	−1	−1	−1	2		
B_{1u}	1	1	−1	−1	−1	−1	1	1	4	T_z	
B_{2u}	1	−1	1	−1	−1	1	−1	1	6	T_u	
B_{3u}	1	−1	−1	1	−1	1	1	−1	6	T_x	

Table 2. Characters, selection rules and group correlations for the fragment 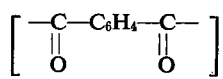 in PET on the basis of C_{2v} symmetry

$V_h \equiv D_{2h}$	$C_{2v}[C_2(z)]$	E	$C_2(z)$	$\sigma_v(zx)$	$\sigma_v(yz)$	n		
A_g, B_{1u}	A_1	1	1	1	1	11	T_z	$\alpha_{xx}, \alpha_{uu}, \alpha_{zz}$
B_{1g}, A_u	A_2	1	1	−1	−1	8	R_z	α_{xu}
B_{2g}, B_{3u}	B_1	1	−1	1	−1	7	$T_x R_u$	α_{zx}
B_{3g}, B_{2u}	B_2	1	−1	−1	1	10	$T_u R_x$	α_{uz}

Table 3. Characters and selection rules for the fragment [—O—CH_2CH_2—O—] of *trans* configuration in PET on basis of C_{2h} symmetry

C_{2h}	E	$C_2(z)$	i	σ_h	n						
A_g	1	1	1	1	5	R_z		α_{xx},	α_{yy},	α_{zz},	α_{xy}
B_g	1	−1	1	−1	4	R_x	R_y		α_{yz},	α_{zx}	
A_u	1	1	−1	−1	4	T_z					
B_u	1	−1	−1	1	5	T_x	T_y				

Table 4. Characters and selection rules for the fragment [—O—CH_2CH_2—O—] of *gauche* configuration on basis of C_2 symmetry

C_2	E	$C_2(y)$	n							
A	1	1	10	T_z		R_z		α_{xx},	α_{yy},	α_{zz},	α_{xy}
B	1	−1	8	T_x,	T_y;	R_x,	R_y		α_{yz},	α_{zx}	

In amorphous regions of the polymer, however, the strict selection rules for V_h symmetry are likely to break down. This would occur when the two C=O groups are no longer strictly related by a centre of symmetry, due to departure from planarity of the terephthalate framework, and a significant reduction to C_{2v} symmetry would be expected. In highly oriented crystalline polymer the restraining influence of the crystal field effect is expected to be considerable, and since the molecule would be virtually fully extended along the fibre axis the relatively high symmetry of the near-planar terephthalate fragment[11] is understandable. In amorphous regions the restraining influence of crystal field effects and selective orientation will be almost totally absent and the chain orientation will be completely random with respect to a hypothetical fibre axis, and accompanied by multiple chain bending and twisting. As a result, the Raman active A_g, B_{2g} and B_{3g} modes of V_h symmetry are expected to appear weakly in amorphous polymer. A significant decrease in intensity of such bands would then be expected with increasing orientation and crystallinity of the polymer. In *Table 9* the suffix 'a' has been added to those modes expected to show such 'amorphous' origin. Likewise, the infra-red active B_{1u}, B_{2u} and B_{3u} modes of V_h symmetry are likely to decrease in intensity with decreasing crystallinity and orientation. Such bands are principally associated with the essentially planar terephthalate framework and are thus designated 'c' in *Table 9* to denote their essentially crystalline origin.

The eight infra-red inactive modes corresponding to the B_{1g} and A_u species of V_h symmetry and the A_2 species of C_{2v} symmetry will not be observed in PET. Only a reduction of the symmetry of the terephthalate framework to C_2 would render the modes active, and this symmetry is not considered feasible.

Frequency notation

The numbering of the frequencies in benzene given in *Table 10* due to Pitzer and Scott[14], is not current frequency notation and is not strictly relevant when applied to the terephthalate framework. The preferred notation of *Table 9* is in keeping with the current practice of numbering modes in order of decreasing frequency within a particular species. The notation also facilitates the numbering of all the normal modes of the polymer repeat unit, and the skeletal vibrations involving chain bending and twisting.

Also summarized in *Table 9* is the predicted infra-red dichroism for each infra-red active mode, determined from the group orientation results for oriented crystalline PET[5] on the basis of the X-ray diffraction results[11]. On reduction from a V_h configuration to a C_{2v} configuration the polarizations are expected to remain as indicated in *Table 9*, but the extent of the polarization will probably vary appreciably between the two configurations.

ASSIGNMENT OF THE NORMAL MODES OF THE FRAGMENT

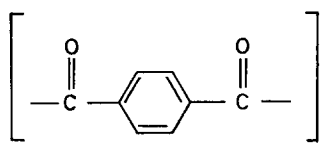

The preceding section dealt with the prediction of the spectrum of the —(CO)—C_6H_4—(CO)— fragment in PET on the basis of an essentially V_h symmetry in fully oriented crystalline polymer, and a significant reduction to C_{2v} symmetry in unoriented amorphous polymer, was expected. Examination of the spectra has revealed that almost all bands of medium intensity observed in the biaxially and uniaxially drawn heat crystallized material have medium to very weak counterparts in the spectrum of the amorphous polymer, and vice versa, and bands having 'amorphous' or 'crystalline' origin could be readily identified. Density measurements show that the extent of crystallization in the PET samples examined increased in the order: amorphous ($\rho = 1{\cdot}34$ g/cm^3)—uniaxially drawn (no heat treatment) ($\rho = 1{\cdot}36$ g/cm^3)—uniaxially drawn, heat crystallized ($\rho = 1{\cdot}39$–$1{\cdot}40$ g/cm^3). The density of completely crystalline PET at room temperature determined by X-ray analysis[15] is 1·46 g/cm^3. Consequently very weak bands of amorphous origin occurring in the spectra of the uniaxially drawn samples are due to the presence of amorphous material which is known to persist up to 40 per cent in heat crystallized unoriented specimens and in PET induced to crystallize in solvent, and up to almost 20 per cent in oriented, annealed samples[15]. Similarly, crystalline bands occurring very weakly in the amorphous film are attributed to the crystalline material formed during cooling. Bands of either crystalline or amorphous origin are observed over the entire infra-red region of the PET spectrum (*Tables 5* and *6*).

Most of the ring vibrations of the terephthalate framework are not likely to differ significantly from those observed in benzene. The assignments of the normal modes of *p*-xylene, H_3C—C_6H_4—CH_3 will also act as a guide in assigning the normal modes of the fragment [—OC—C_6H_4—CO—].

Further information is given by the assignments of the corresponding 'terephthalate' modes in *cis*- and *trans*-poly(cyclohexane-1,4-dimethylene terephthalate), (PCHT)

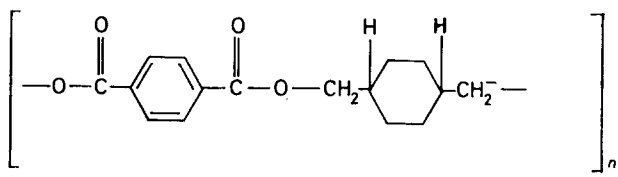

which has been examined in the conventional infra-red by Boye[16]. This structure differs from that of PET in having a cyclohexane ring between the two methylene groups of PET. No appreciable frequency shifts from those in PET for ν_1–ν_{36} are expected for this polymer, and the 'terephthalate' modes common to each polymer are expected to exhibit similar origin and polarization. *Table 8* lists all the absorption maxima which occur at similar frequencies and intensities in both PET and PCHT. Nearly all absorptions common to both polymers have the same polarization and show the same intensity changes upon crystallization in each case. The majority of these common bands can be attributed to the terephthalate framework

Table 5. Far infra-red spectrum of polyethylene terephthalate

Biaxially oriented. Crystallized	*Uniaxially oriented. Crystallized* ⊥	*Uniaxially oriented. Crystallized* ∥	*Biaxially oriented. Uncrystallized*	*Uniaxially oriented. Uncrystallized* ⊥	*Uniaxially oriented. Uncrystallized* ∥	*Amorphous*	P	O	*Assignment*
						36 vvw			
50 vvw	52 vvw	51 vvw	54 w, b	47 vw	46 vw	46 vw	π	a	$\tau^{\parallel}_{CCOC}$ (59′, *B*; 59, A_g)
62–80 m, b	64 vw / 71 vvw	61 vw / 74 vw	70 w, b	59 vvw / 73 vw	62 vvw / 73 vw	58 vw / 68 vvw	σ / σ	c? / c	$\tau^{\parallel}_{CCOC}$ (58′, B)
95–108 vw, sh	97 w / 109 vw	95 w / 107 vw	~ 90 w, sh	95 vvw / 112 vvw	95 vvw / 111 vvw	95 vw, sh / 117 w, b	π	c / a	$\tau_{C_6H_4CO}$ (57, A_g; 57′, *B*)
139 w	146 w	139 w	140 vw	146 vvw	142 vw	138 vvw	π	c	$\delta^{\parallel}_{CCO\perp}$ (62, A_u)
156 w, sh	153 vvw		150–180	155 vvw	154 vvw	155 vvw		c?	$\delta_{C-(C=O)} + \delta_{CH\perp}$ (24, B_{1u})
178 m		177 vw	m, b					c	
193 w, sh	192 vw			189 vw	187 vw	190 m		a	$\delta^{\parallel}_{COC\parallel}$ (56, A_g; 56′, *A*)
217 vw, sh		217 vw				213 vw	σ		$\delta_{C-(C=O)\parallel}$ (36, B_{3u})
235 vvw	234 vw			243 vvw	243 vvw	235 vw		a?	
	252 vvw	259 vvw		~260 vvw, b	~260 vvw, b				$\delta^{\parallel}_{CCO\perp}$ 62′ (*B*)
						274 vvw		a	
						289 w, sh		a	$\delta^{\parallel}_{CCO\parallel}$ 55′ (*A*)
306 w		300 w, b	290 w	304 w, b	304 w, b	295 w, b	π	a	18, B_{3g}; 49, A_u
355 w	358 vw	360 m	355 m	348 m, b	349 m, b	345 m, b	σ		49′, *B*; 56, *A*
379 s	378 m	383 m	381 m	387 m, b	381 m, b	387 vw		c	$\delta^{\parallel}_{COC\perp}$ (61, A_u; 61′, *B*)
				417 vw	417 vw	417 w		a	
422 vw	425 m		424 vw	424 m	426 m	423 m	σ		$\delta_{CCC\perp}$ (23, B_{1u})
435 m		432 m	434 m	434 w	435 m	434 vw	π	c	$\delta_{CCO\parallel}$ (54′, *A*)
458 vw								c	$\delta^{\parallel}_{CCO\parallel}$ (55, A_g)
474 vvw								c	
504 m	501 m	502 m	503 m	500 m	499 m	498 m	π	c	$\delta_{CCO\parallel}$ (54, B_u)
518 w		519 m	520 m	520 w	520 m	518 m	π		$\delta_{C=O\perp}$ (22, B_{1u})
546 w		551 vw	545 w				π?	c	
	571 w		566 m	568 vw			π	c	
		584 w	585 w					c	
	618 vw		613 vw	613 vw	613 vw	613 w	π?	a	
630 vw	630 m	630 m	630 vw	630 w	630 w	632 w	π		$\omega_{C=O}$ (35, B_{3u})

Table 6. Infra-red spectrum of poly(ethylene terephthalate)

Biaxially oriented. Crystallized	*Uniaxially oriented. Crystallized*	*Biaxially oriented. Uncrystallized*	*Uniaxially oriented. Uncrystallized*	*Amorphous*	P	O	*Assignment*
		645 w		645 w, b		a	$\delta_{C=O\perp}(17, B_{3g})$
669 w, b	669 w, sh	669 vw	671 w, sh		π?	c	
	678 w	680 w	680 w	680 w	σ?	a	$\delta_{CCC\perp}(16, B_{3g})$
709 w, sh	709 m, sh	709 m, sh	712 m, sh	709 m, sh	σ	a	$\delta_{C-(C=O)}+\delta_{CH\perp}(21, B_u)$
730 vs	730 vs	730 vs	730 vs	730 vs	σ		
		775 w, sh	775 vvw	775 vvw		a	$\delta_{CH\perp}(14, B_{3g})$
794 m	794 m	794 m	794 w	794 m	π		$\nu_{CC}(6, A_g)$
				810 w		a	
852 s	846 m	847 s	847 m, sh	843 m	π	c	$\rho_{CH_2}(48, A)$
873 m	873 m	872 s	870 s	869 s	σ	a	$\nu_{CC}(41', A)$
897 w	896 w	897 w	896 w, sh	893 s, sh	π?	a	$\rho_{CH_2}(48', A)$
				939 vvw		a	$\delta_{CH\perp}(15, B_{3g})$?
971 s	971 m	970 s	971 s	971 s	π		$\delta_{CCC\parallel}(30, B_{2u})$
1019 s	1015 s	1019 s	1031 s	1015 s	π		$\delta_{CH\parallel}(29, B_{2u})$
1038 m	1041 s	1042 m		1041 s		a	$\nu_{s\,C-O}(40', A)$
1100 vs	1100 vs	1100 vs	1100 vs	1100 vs	π	a	$\nu_{as\,C-O}(53, B)$
1120 vs	1120 vs	1120 vs	1120 s	1120 m	π	c	$\nu_{as\,C-O}(53, B_u)$
1171 w	1174 m	1175 vw	1174 m	1174 m	π?	a	$5A_g/34B_{3u}$
1248 sh	1248 sh	1248 sh	1248 sh	1248 sh	π	a	$\nu_{s-\overset{\parallel}{C}-O}$, 60', 60
1266 vs	1266 vs	1265 vs	1266 vs	1266 vs	π	c	
1335 m	1335 m	1336 m	1335 m	1335 m	π		$\nu_{C-(C=O)}$, ω_{CH_2}
1364 vw	1368 w	1371 vw	1368 w	1369 m	π?	a	ω_{CH_2} [52', B]
1377 vw		1377 vvw	1377 sh	1377 sh		a?	$\nu_{C-(C=O)}$ [4, A_g]
1405 w	1399 w	1408 w	1399 w	1407 m	π	a	δ_{COH} end groups
1435 w	1435 w	1435 w	1435 w	1435 w		a	$\delta_{CH_2}(38', B)$

Table 6—continued

Biaxially oriented. Crystallized	*Uniaxially oriented. Crystallized*	*Biaxially oriented. Uncrystallized*	*Uniaxially oriented. Uncrystallized*	*Amorphous*	P	O	*Assignment*
1449 w	1447 w	1451 w	1447 w	1448 w	π	a	δ_{CH_2} [51′, *B*]
1468 w	1468 w	1471 m			σ	c	33, B_{3u}/51, B_u
1497 w	1497 m	1502 w	1502 w	1502 w	π		ν_{CC} (27, B_{2u})
1515 vvw	1518 vvw	1518 vvw	1529 vw	1524 vvw			ν_{CC} (32, B_{3u})
1570 vw	1577 w	1579 w	1580 w	1577 m	π	a	ν_{CC} (3, A_g)
1610 vw	1610 w	1613 vw	1613 w	1613 w	σ	a?	$\nu_{sC=O}$ (2, A_g)
1681 vw	1699 vvw	1689 vvw				c	
1721 vs	1709 vs	1716 vs	1709 vs	1715 vs	σ		$\nu_{asC=O}$ (26, B_{2u})
1815 w	1815 w	1812 w	1815 m	1812 w	π		852 (A_u)+971 (B_{2u})
		1835 w					=1823
		1859 w					
				1908 vw		a	
1957 w	1957 m	1959 w	1957 w	1949 w	σ		977 (A_u)+1016 (B_{3g})
2079 w						c	=1993
	2114 w	2114 w	2105 w	2114 w	π		
2183 vw						c	
	2230 w		2217 vvw	2237 vw			
	2252 w	2268 w	2252 vvw				
2288 vw	2288 vw		2283 vw	2283 vw			
2353 vvw	2342 vvw			2331 vvw			
	2381 w	2370 w	2370 w	2381 vw			

Table 6—continued

Biaxially oriented. Crystallized	*Uniaxially oriented. Crystallized*	*Biaxially oriented. Uncrystallized*	*Uniaxially oriented. Uncrystallized*	*Amorphous*	P	O	*Assignment*
2410 vw						c	
	2457 vvw					c?	
	2500 vvw	2500 vw				c?	
2545 vw	2532 m		2545 w	2532 vw			
	2564 w					c	
	2625 vw	2604 vw	2625 vvw	2625 vvw			
2674 vw	2674 vvw					c	
	2725 vvw	2732 vw				c?	
	2762 vw		2770 vw	2755 vw			
2801 vw	2809 vw	2817 vvw	2809 vw	2809 vw			
2852 vw	2852 vw	2852 vw	2852 w	2852 w	π		$\nu_{s\,CH_2}(50, B_u)$
2890 vw			2890 m	2882 w	π	a	$37'(A)/50'(B)$
	2899 w	2907 w				c	$\nu_{as\,CH_2}(46, A_u)$
2967 w	2967 m	2967 m	2959 s	2967 s	π	a	$42'A/46'B$
3012 w	3012 w	3012 vw	3012 w		π?	c	
3058 vw	3058 w		3049 w	3058 w	π	a?	$\nu_{CH}(25, B_{2u})$
		3068 w					$\nu_{CH}(1, A_g)$
	3096 vvw		3086 vvw	3096 vw	σ	c?	$\nu_{CH}(25, B_{2u})$
	3115 vvw				σ	c	
3185 vw	3165 vvw	3195 vw					
	3215 vvw		3215 vvw	3226 vvw			
3300 vw	3300 vw	3311 vw	3290 vvw	3300 vvw	σ?		
	3333 vw		3333 vvvw	3333 vvw			
3431 w	3431 m	3425 w	3425 m	3431 w	σ	c	$2\times\nu_{C=O}=3442$
3546 vw	3546 w	3546 w	3534 w	3546 vw	π		$\nu_{s\,(OH)}$ (end groups)

Table 7. Infra-red spectra and frequency correlations of some model compounds of poly(ethylene terephthalate)

Terephthalic acid	*Ethylene glycol*	*Ethylene glycol terephthalate 'monomer'*	*Ethylene glycol terephthalate oligomer*	*Ethylene glycol dibenzoate*	*PET amorphous*	*Assignment*
				48 vw	46 vw	$\tau^{\parallel}_{COCC}\,\nu_{59}\,(A_g)$, $\nu'_{59}\,(B)$
		59 vvw	57 vvw	59 vvw	58 vw	
			71 vvw	70 vw	68 vvw	$\tau_{CCOC}\,\nu_{58}\,(A_g)$, $\nu'_{58}\,(B)$
		83 vvw	83 vw	83 vvw		
89 vvw?						?
				93 w	95 vw	$\tau_{C_6H_4CO}\,\nu_{57}\,(A_g)$, $\nu'_{57}\,(B)$
			102 vw			
110 vw		115 vw	115 vvw	117 vw	117 w, b	
123 vvw		128 vw	124 vvw			
			138 w	149 vw	138 vvw	$\delta^{\parallel}_{CCO\perp}\,62\,(A_u)$
			155 vvw		155 vvw	$\nu_{24}\,(B_{2u})$
200 vw		177 vvw		181 vw	190 m	$\delta_{C-(C=O)\perp}/\delta^{\parallel}_{COC\parallel}$
				200		
				211 w	213 vw	
225 w		229 w	234 m	235 m	235 vw	$\delta_{C-(C=O)\parallel}\,(36)$
243 m						
				259 vw	259 vvw*	$\delta^{\parallel}_{CCO\perp}$, $\nu'_{62}\,(B_u)$
263 vvw?		275 w			274 vvw	
		282 w	280 w		289 w	$\delta^{\parallel}_{CCO\perp}$, $\nu'_{55}\,(A)$
295 w		306 w	308 w	308 vw	295 w, b	$\delta_{C-(C=O)\perp}\,(18)$
321 m		327 vw		326 vvw		
				339 vw		
352 w	352 w	353 w		350 w	345 m, b	$\delta_{CCO\parallel}/\delta_{CCC\perp}$
		382 m			387 vw	$\delta_{CCC\perp}/\delta^{\parallel}_{COC\perp}$
409 vvw				400 w	417 w	$\delta_{CCC\parallel}\,(7)$

Table 7—continued

Terephthalic acid	*Ethylene glycol*	*Ethylene glycol terephthalate 'monomer'*	*Ethylene glycol terephthalate oligomer*	*Ethylene glycol dibenzoate*	*PET amorphous*	*Assignment*
			418 m		423 m	$\delta^{\parallel}_{COC\perp}\ \nu'_{61}$ (*B*)
		431 w	434 vw		434 vw	
		438 vw				
447 m						$\delta_{CCC\parallel}$?
	478	486 w	484 w	475 vw	474 vvw*	$\delta_{CCO\parallel}$ (54′)
490 m		495 vw	496 w		498 m	$\delta_{C=O\perp}$ (49)
	500					
500 w		508 w	513 vw		518 m	$\delta_{CCO\perp}$ (22)
525 m		523 vw				
562 m		551 vwb		564 vw	546 w*	
610 vw		615 w	615 w	615 vw	613 w	$\delta_{C=O\perp}$ (17)
630 vw		630 w	630 w		632 w	$\delta_{C=O\parallel}$ (35)
		645 vw	641 vw		645 w, b	
670 vw				670 vw		
685 w		685 sh		681 w	680 w	$\delta_{CCC\perp}$ (16)
		709 m	709 m?	709 m	709 m	$\delta_{CCC\parallel}$ (30)
731 m		725 m	722 m		730 vs	$\delta_{[C-CO+CH]\perp}$ (21)
781 m					775 vvw	$\delta_{CH\perp}$ (14)
		794 vw	790 vw	800 vw	794 m	
833 vw		817 vw			810 w	$\nu_{CC}\ \nu_6$ (A_g)
		833 vw				
	(900)	858 vw	844 w	850 w	843 m	$\rho_{CH_2}\ \nu_{48}$ (A_u)
	864 m	870 vw	869 m		869 s	ν_{CC} [41′, *A*]
880 m						$\delta_{CH\perp}$
		889 vw	895 w, b	905 m	893 s	ρ_{CH_2} [48′, *A*]

Table 7—continued

Terephthalic acid	*Ethylene glycol*	*Ethylene glycol terephthalate 'monomer'*	*Ethylene glycol terephthalate oligomer*	*Ethylene glycol dibenzoate*	*PET amorphous*	*Assignment*
	887 s					
935 s						$\delta_{OH\perp}$
	(1061)	900 vvw		937 vvw	939 vvw	$\rho_{CH_2}\nu_{15}/\nu'_{44}$
980 vvw		967 vw	968 w	980 w	971 m	$\delta_{CCC\parallel}\ \nu_{30}(B_{2u})$
995 vvw						$\delta_{CH\perp}$
1017 w		1013 w	1017 m	1020 w	1015 s	$\delta_{CH\parallel}\ \nu_{29}(B_{2u})$
	1038 s	1064 w	1043 w	1048 vw	1041 s	$\nu_{s\ C-O}\ \nu'_{40}(A)$
1078 vw						
	1087 vs	1101 vw	1100 vs	1100 s	1100 vs	$\nu_{as\ C-O}\ \nu'_{53}(B)$
1110 w		1124 w	1120 m	1120 m	1120 m	$\nu_{as\ C-O}\ \nu_{53}(B_u)$
1134 w						
1183 w			1174 w	1175 w	1174 m	$\delta_{CH\parallel}\ \nu_5/\nu_{34}$
					1248 sh	$\nu^{\parallel}_{C-O}60'/60$
1282 s	1260 vw	1264 m	1265 vs	1265 s	1266 vs	
1320 sh						ν_{CC}
		1335 vw	1340 m	1337 m	1335 m	ν_{CC}, ω_{CH_2}
	1332					
1380 w		1370 vw	1370 w	1365 m	1369 m	$\omega_{CH_2}(52', B)$
	1370 m		1382 w		1377 sh	$\nu_{C-(C=O)}[4, A_g]$
1414 m	1405 m, b	1405 vw	1407 m		1407 m	δ_{COH}
			1435 vw	1435 vw	1435 w	$\delta_{CH_2}\nu'_{38}(B)$
	1459 m	1447 vw	1450 w	1450 w	1448 w	
1458 m						$\nu_{51'}(B)$
	(1510)	1464 vvw	1469 w	1468 w	1468 w	$\nu_{CC}/\delta_{CH_2}\nu_{33}/\nu_{51}$
1511 w		1495 vw	1502 w	1500 w	1502 w	$\nu_{CC}\nu_{27}(B_{2u})$
		1515 vvw	1522 vvw	1523 vvw	1524 vvw	$\nu_{CC}\nu_{32}(B_{2u})$

Table 7—continued

Terephthalic acid	*Ethylene glycol*	*Ethylene glycol terephthalate 'monomer'*	*Ethylene glycol terephthalate oligomer*	*Ethylene glycol dibenzoate*	*PET Amorphous*	*Assignment*
1567 w			1575 w	1580 w	1577 m	$\nu_{CC}\nu_3(A_g)$
1613 w		1613 vvw	1610 vvw		1613 w	$\nu_{s\,C=O}\nu_2(A_g)$
1672 s		1701 m	1715 vs	1707 vs	1715 vs	$\nu_{as\,C=O}\nu_{26}(B_{2u})$
				1725 vs		
1812 w				1814 w	1812 w	
1898 vw				1893 w	1908 vw	
1957 vw		1953 vw	1945 vvw 1957 vw	1955 vw	1949 w	
2066 vw					2079 w	
2114 vw			2110 vw		2114 w	
2222 vvw			2240 vvw	2240 vvw	2237 vw	
2353 vw			2350 vw	2330 vw	2353 vvw	
2530 m			2570 vvwb	2520 vw	2500 vw	$\nu_{as\,OH}$
2646 m				2635 vvw	2625 vvw	$\nu_{as\,OH}$
2860 s				2850 w		$\nu_{s\,CH_2}\nu_{50}(B_u)$
	(2850)					
	2875 s	2874 vvw	2885 vvw	2880 w	2882 w	$\nu_{s\,CH_2}\,37'/50'$
	(2940)	2924 vvw	2905 vw	2910 vw	2907 w	$\nu_{as\,CH_2}\nu_{46}(A_u)$
2916 vs						
	2935 s	2967 vw	2965 w	2967 w	2967 s	$\nu_{as\,CH_2}\nu'_{42}/\nu'_{46}$
	2938 s	3023 vvw	3005 vvw	3020 vvw	3012 w	$\nu_{a\,CH_2}$
3058 m				3060 vw	3058 w	$\nu_{CH}\,\nu_{25}(B_{2u})$
3096 vw			3100 vvw		3096 vw	$\nu_{CH}\,\nu_{31}(B_{2u})$
					3115 vvw	
3413 vvw		3425 w	3425 w, b	3430 w, b	3431 w	$\nu_{s\,O-H}$
3546 vvw		3521 w	3520 w, b		3546 vw	

* Band observed only in crystalline PET.
() Calculated frequency for *trans* configuration—see text.
The numbered frequencies correspond approximately to those of the PET repeat unit—see text

Table 8. Infra-red bands common to both PET and PCHT

PET			PCHT				
cm^{-1}	P	O	cm^{-1}	P	O	I*	*Assignment*
73 vw	σ	c	73 w	σ	c		$\tau_{CCOO}^{\parallel}(B_{2g})$
117 w, b	π	a	112 vw	π			$\tau_{(C_6H_4)CO}^{\parallel}$
156 w		c	158 vw	π?			$\delta_{C-(C=O)}+\delta_{CH\perp}\nu_{24}(B_{1u})$
178 m	π	c	175 w, b	π	c?		$\delta_{COC\parallel}^{\parallel}$
235 vw	σ		240 vvw	σ			$\delta_{C-(C=O)\parallel}(\nu_{36}, B_{3u})$
295 w	π	a	294 m	π			$\delta_{C-(C=O)\perp}(\nu_{18}, B_{3g})$
379 s	π	c	394 vw		c	*trans*	$\delta_{COC\perp}^{\parallel}$
417 w		a	408 m	π	a		$\delta_{CCC\parallel}(\nu_7, A_g)$
423 m	σ		424 w	σ			$\delta_{CCC\perp}(\nu_{23}, B_{1u})$
504 m	π	c	497 m				$\delta_{CCO\parallel}$
518 w	π		515 w, b				$\rho_{C=O}(\nu_{22}, B_{1u})$
546 w	π?	c?	552 w		a?		
630 vw	π		631 w	π		*cis*	$\omega_{C=O}(\nu_{35}, B_{3u})$
645 w		a	645 vw	π		*cis*	
680 w	σ?	a	675 vvw	σ?	a?		$\delta_{CCC\perp}(\nu_{16}, B_{3g})$
709 sh	σ?	a	705 sh				
730 vs	σ		729 s	σ			$\delta_{C-(C=O)}+\delta_{CH\perp}(\nu_{21}, B_{1u})$
775 vvw		a	770 vw		a?		$\delta_{CH\perp}(\nu_{14}, B_{2g})$
794 m	π	?	795 w	π	a?	}	$\nu_{CC}(\nu_6, A_g)$?
810 w		a	802 vvw		a	}	
852 s	π	c	850 vw	σ	c		ρ_{OH_2}
939 vvw		a	930 sh			*cis*	$\delta_{CH\perp}(\nu_{15}, B_{3g})$

Table 8—continued

PET			PCHT				
cm^{-1}	P	O	cm^{-1}	P	O	I*	*Assignment*
971 s	π	c	966 m	π			$\delta_{CCC\parallel}$ (ν_{30}, B_{2u})
1019 s	π		1012 m	π			$\delta_{CH\parallel}$ (ν_{29}, B_{2u})
1100 vs	π	a	1107 vs	π			$\nu_{as\ C-O}$
1120 vs	π	c	1119 vs	π			$\nu_{as\ C-O}$
1174 m	π?	a	1168 w				$\delta_{CH\parallel}$ (ν_5, A_g)/(ν_{34}, B_{3u})
1248 sh	π	a	1253 vs	π			$\nu_{s\ \overset{\parallel}{C}-O}$
1266 vs	π	c	1263 vs	π			$\nu_{s\ \overset{\parallel}{C}-O}$
1335 m	π	c	1330 sh			*cis*	$\nu_{C-(C=O)}/\omega_{CH_2}$
1369 m	π?	a	1370 m	π	a		ω_{CH_2}
1407 m	π	a	1402 m	π			δ_{COH} (end groups)
1468 w	σ	c	1456 m	σ			ν_{CC} (ν_{33}, B_{3u})
1497 w	π		1499 m	π			ν_{CC} (ν_{27}, B_{2u})
1515 vvw			1520 vw	π?	c?		ν_{CC} (ν_{32}, B_{3u})
1577 m	π	a	1583 w	π?	a		ν_{CC} (ν_3, A_g)
1613 w	σ	a?	1616 w	σ			$\nu_{s\ C=O}$ (ν_2, A_g)
1715 vs	σ		1717 vs	σ			$\nu_{as\ C=O}$ (ν_{25}, B_{2u})
1815 sh	π		1815 sh	π	c		
3058 vw	π		3068 vw				ν_{CH} (ν_{25}, B_{2u})
3096 vw	σ	c?	3085 vvw				ν_{CH} (ν_{31}, B_{3u})
3115 vvw	σ	c	3115 vvw				
3431 w	σ	c	3416 w	σ			$\nu_{s\ OH}$ (end groups)

I* isomer (*cis*/*trans*); bands not identified as being due specifically to *cis*- or *trans*-isomer are common to both stereo-isomers.

in both polymers and thus *Table 8* is a considerable aid to the assignment of the normal modes of the 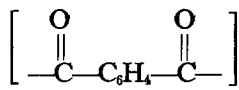 fragment. The structure of PCHT will be discussed elsewhere.

Table 9 summarizes the frequencies assigned as normal modes of the terephthalate fragment in this investigation in both PET and PCHT and *Table 10* gives the corresponding values assigned to *p*-xylene[14] and benzene[17,18]. The assignment of the normal modes for each symmetry species will now be discussed.

A_g species

The A_g species of V_h symmetry is inactive in the infra-red, but the modes are expected to appear weakly in the infra-red on reduction to C_{2v} symmetry, giving rise to bands of 'amorphous' origin. Consequently, on the basis of the model discussed earlier, the bands will be virtually absent in highly oriented and crystalline specimens. All the A_g modes are expected to exhibit π polarization apart from the C=O in-phase stretching vibration which will display σ polarization.

The C—H symmetric in-phase stretching mode (ν_1) is assigned to the weak amorphous π band in both polymers at 3 068 cm^{-1}. In benzene and *p*-xylene the mode occurs at 3 062 cm^{-1}.

The amorphous π band common to PET and PCHT at $\sim$ 1 577 cm^{-1} is attributed to the C—C symmetric stretching in the benzene ring (ν_3). Corresponding values are, in terephthalic acid, 1 567 cm^{-1}, benzene, 1 596 cm^{-1} and *p*-xylene, 1 616 cm^{-1}.

The C—(C=O) symmetric in-phase stretching mode is expected in the region 1 300–1 400 cm^{-1}; the bond might be expected to display some double bond character due to resonance caused by the presence of the carbonyl group in conjugation with the aromatic ring, and the frequency is then likely to lie midway between that for C—C and C=C. In terephthalic acid weak absorption at 1 380 cm^{-1} is attributed to this bond stretching. The only band of definite amorphous origin which can be reasonably assigned to ν_4 is the π band common to both polymers at $\sim$ 1 370 cm^{-1}. The apparent shift of this band upon deuteration of the glycol residue[7] and its subsequent assignment to the latter[6] is more complicated than previously supposed since the band is resolved into two components at $\sim$ 1 368 and 1 377 cm^{-1}, the latter shifting and presumably merging upon deuteration with the strong 1 335–1 266 cm^{-1} complex, and the former shifting to $\sim$ 1 380 cm^{-1}. The aromatic ring breathing mode (ν_6) occurs in benzene at 992 cm^{-1} (ν_1, A_{1g}). The introduction of two methyl groups as para substituents lowers the frequency to 826 cm^{-1} in *p*-xylene. Consequently the weak band observed only in the amorphous spectra of both polymers at 810 cm^{-1}, of unknown polarization, is tentatively assigned to ν_6. In terephthalic acid and bis-β-hydroxyethyl terephthalate ('monomer') absorption occurs at 833 and 817 cm^{-1}, which is attributed to the same mode. The medium π band present in both polymers at $\sim$ 795 cm^{-1} is found to decrease very slightly upon drawing and crystallization of amorphous specimens. Its intensity in crystal-

line specimens of both polymers prevents us from assigning this band to ν_6 (A_g) although it shows the correct parallel dichroism and frequency expected for this ring stretching mode.

The weak amorphous bands at 417 cm^{-1} in PET and 408 cm^{-1} (π) in PCHT are tentatively assigned to the ring C—C—C in-plane bending mode (ν_7). In benzene the corresponding mode (ν_{6A}, E_{2g}) occurs at 606 cm^{-1} and is lowered to 460 cm^{-1} in *p*-xylene by the methyl para substituents. In terephthalic acid and ethylene glycol dibenzoate similar absorption occurs at 409 and 400 cm^{-1} respectively.

Two modes now remain to be assigned. The very intense σ band at 1 721 cm^{-1} will be assigned to $\nu_{as\,C=O}$ (out-of-phase) [ν_{26}, (B_{2u})]. The C=O stretching vibration should exhibit σ polarization. Normally ester C=O groups conjugated with aromatic rings absorb strongly at 1 740–1 715 cm^{-1}. The extent of the coupling between the two carbonyls is likely to be only slight but since the planar terephthalate framework is a conjugated system, perturbation between the two carbonyls could lower $\nu_{s\,C=O}$ (in-phase) significantly. The amorphous σ band at 1 613 cm^{-1} is then assigned to this mode. In terephthalic acid the strong absorption due to $\nu_{as\,C=O}$ occurs at 1 672 cm^{-1} and $\nu_{s\,C=O}$ is believed to occur at 1 613 cm^{-1}, although it has been tentatively assigned to a ring mode[19]. The analogy must, nevertheless, be made with caution since hydrogen bonding may complicate the system in terephthalic acid. A weak band is observed, however, in ethylene glycol terephthalate ('monomer' and oligomer) at 1 613 cm^{-1}.

Finally, the C—H in-plane bending mode, ν_5, is expected in the region 1 100–1 200 cm^{-1}. In benzene the mode (ν_{9A}, E_{2g}) is believed to occur at 1 178 cm^{-1} and in *p*-xylene at 1 182 cm^{-1}. ν_5 is therefore assigned to the amorphous π bands occurring in both polymers at 1 170 cm^{-1}.

B_{1g} and A_u species

These two species are inactive in the infra-red in both the V_h and C_{2v} configurations of the terephthalate framework.

B_{2g} species

The single mode belonging to this species, C—H out-of-ring-plane deformation (ν_{14}) is infra-red active only on reduction to C_{2v} symmetry. It will exhibit perpendicular dichroism with respect to the plane of the benzene ring. In benzene and *p*-xylene the corresponding modes occur at 849 and 811 cm^{-1} (ν_{10A}, E_{1g}). Consequently, the amorphous bands of unknown polarization at $\sim$ 775 cm^{-1} are tentatively assigned to the mode in PET and PCHT.

B_{3g} species

The four vibrations belonging to this species become infra-red active only on reduction to C_{2v} symmetry. All are expected to exhibit perpendicular dichroism (pleochroism) with respect to the plane of the film, and all will be of amorphous origin, decreasing sharply in intensity upon crystallization. Since the crystallinity of amorphous material increases with biaxial orientation, the 'amorphous' modes corresponding to the B_{3g} species of

Table 9. Assignment of fundamental modes of vibration of the fragment —C(=O)—C_6H_4—C(=O)— in PET and PCHT on the basis of V_h/C_{2v} symmetries

$D_{2h} \equiv V_h$	$C_{2v}[C_2(z)]$	*No.*		P	O	PET	PCHT	*Assignment*
A_g	A_1	1		π	a	(3068)	(3068)	$\nu_{s\,C-H}$
		2	s	σ	a	(1613)	(1616)	$\nu_{s\,C=O}$
		3	s	π	a	(1577)	(1583)	$\nu_{s\,C-C}$
Raman, *P*	Raman, *P*	4		π	a	(1377)	(1370)	$\nu_{s\,C-(C=O)}$
	Infra-red	5	s	π	a	(1174)	(1168)	$\delta_{C-H\parallel}$
		6	s	π	a	(810)	(802)	$\nu_{s\,C-C}$
		7	s	π	a	(417)	(408)	$\delta_{C-C-C\parallel}$
B_{1g}	A_2	8		—	—	—	—	$\nu_{as\,C-H}$
		9		—	—	—	—	$\delta_{C-H\parallel}$
		10	s	—	—	—	—	$\nu_{as\,C-C}$
Raman	Raman	11	s	—	—	—	—	$\omega_{C=O}$
dp	*dp*	12	s	—	—	—	—	$\delta_{C-C-C\parallel}$
		13	s	—	—	—	—	$\delta_{C-(C=O)\parallel}$
B_{2g}	B_1	14		σ	a	(775)	(770)	$\delta_{C-H\perp}$
Raman	Raman							
dp	*IR*							
B_{3g}	B_2	15		σ	a	(939)	(930)	$\delta_{C-H\perp}$
		16	s	σ	a	(680)	(675)	$\delta_{C-C-C\perp}$
Raman	Raman	17	s	σ	s	(645)	(645)	$\rho_{C=O}$
dp	*IR*	18	s	σ	a	(295)	(294)	$\delta_{C-(C=O)\perp}$

Table 9—continued

$D_{2h} \equiv V_h$	$C_{2v}[C_2(z)]$	*No.*		P	O	PET	PCHT	*Assignment*
A_u	A_2	19		—	—	—	—	$\delta_{C-H\perp}$
		20	s	—	—	—	—	$\delta_{C-C-C\perp}$
i.a.	Raman							
B_{1u}	A_1	21		σ	c	730	729	$\delta_{C-(C=O)\perp} + \delta_{C-H\perp}$
		22	s	σ	c	518	515	$\rho_{C=O\perp}$
	Raman	23	s	σ	c	423	424	$\delta_{C-C-C\perp}$
IR	*IR*	24	s	σ	c	155	158	$\delta_{C-(C=O)\perp} + \delta_{C-H\perp}$
B_{2u}	B_2	25		π	c	3058	3068	$\nu_{s\,C-H}$
		26	s	σ	c	1721	1717	$\nu_{as\,C=O}$
	Raman	27	s	π	c	1497	1499	$\nu_{s\,C-C}$
IR	*IR*	28	s	π	c	1335	1330	$\nu_{as\,C-(C=O)}$
		29		π	c	1019	1012	$\delta_{C-H\parallel}$
		30	s	π	c	971	966	$\delta_{C-C-C\parallel}$
B_{3u}	B_1	31		σ	c	3096	3085	$\nu_{as\,C-H}$
		32	s	σ	c	1515	1520	$\nu_{as\,C-C}$
	Raman	33	s	σ	c	1468	1456	$\nu_{as\,C-C}$
IR	*IR*	34		σ	c	1171	1168	$\delta_{C-H\parallel}$
		35	s	σ	c	630	634	$\omega_{C=O\parallel}$
		36	s	σ	c	235	240	$\delta_{C-(C=O)\parallel}$

() frequencies in parentheses denote infra-red activity only in C_{2v} symmetry species;
s denotes 'skeletal' vibration; $\parallel$ parallel $\perp$ perpendicular;
P predicted infra-red dichroism in oriented specimen;
O band origin; c crystal; a amorphous.

Table 10. Vibrational modes of the 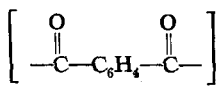 fragment in PET compared to the corresponding modes in *p*-xylene and benzene

Species (V_h)	*No.*		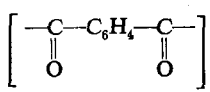	*p-Xylene*	*Benzene*	*No.*	*Species* (D_{6h})	*Assignment*
A_g	1		3068	3062	3062	2	A_{1g}	ν_{CH}
	3	s	1577	1616	1596	8*A*	E_{2g}	ν_{CC}
	4	s	1377	1204	(3047)	7*A*	E_{2g}	ν_{CX}*
	5		1174	1182	1178	9*A*	E_{2g}	$\delta_{CH\parallel}$
	6	s	810	826	992	1	A_{1g}	ν_{CC}
	7	s	417	460	606	6*A*	E_{2g}	$\delta_{CCC\parallel}$
B_{2g}	14		775	811	849	10*A*	E_{1g}	$\delta_{CH\perp}$
B_{3g}	15		939	959	1016	5	B_{2g}	$\delta_{CH\perp}$
	16	s	680	697	683	4	B_{2g}	$\delta_{CCC\perp}$
	18	s	295	313	(849)	10*B*	E_{1g}	$\delta_{CX\perp}$
B_{1u}	21		730	800	(985)	17*B*	E_{2u}	$\delta_{CX}+\delta_{CH\perp}$
	23	s	423	389	400	16*B*	E_{2u}	$\delta_{CCC\perp}$
	24	s	155	170	(671)	11	A_{2u}	$\delta_{CX}+\delta_{CH\perp}$

Table 10—continued

Species (V_h)	*No.*		—C(=O)—C_6H_4—C(=O)—	*p-Xylene*	*Benzene*	*No.*	*Species* (D_{6h})	*Assignment*
B_{2u}	25		3058	3046	3046	20*A*	B_{1u}	ν_{CH}
	27	s	1497	1525	1485	19*A*	E_{1u}	ν_{CC}
	28	s	1335	1200	(3080)	13	E_{1u}	ν_{CX}
	29		1019	1030	1037	18*A*	E_{1u}	$\delta_{CH\parallel}$
	30	s	971	720	1010	12	B_{1u}	$\delta_{CCC\parallel}$
B_{3u}	31		3096	3080	3080	20*B*	E_{1u}	ν_{CH}
	32	s	1515	1640	1693	14	B_{2u}	ν_{CC}
	33	s	1468	1450	1485	19*B*	E_{1u}	ν_{CC}
	34		1171	1100	1170	15	B_{2u}	$\delta_{CH\parallel}$
	36	s	217/235	232	(1037)	18*B*	E_{1u}	$\delta_{CX\parallel}$

s denotes 'skeletal' vibration.

() frequencies in parentheses are where large differences occur between corresponding terephthalate, *p*-xylene and benzene modes due to mass of para substituent X.

* for $\left[-C(=O)-C_6H_4-C(=O)-\right]$ fragment, X = (C=O)

for $H_3C-C_6H_4-CH_3$ X = (CH_3)

for C_6H_6 X = (H)

V_h symmetry become progressively weaker upon orientation. Consequently the dichroism of such bands is exceedingly difficult to assess.

The very weak band occurring only in amorphous PET and PCHT at ~ 939 cm^{-1} is assigned to C—H out-of-plane deformation (ν_{15}). In benzene and *p*-xylene the corresponding modes occur at 1 016 and 959 cm^{-1}, respectively. However, this band might also be due to a CH_2 rocking mode, expected at this frequency, in the glycol or cyclohexanol residue.

The weak amorphous bands at 680 cm^{-1} (believed to have σ polarization) are assigned to ring C—C—C out-of-plane bending (ν_{16}). In benzene, *p*-xylene and terephthalic acid, the corresponding modes are believed to occur at 685, 697 and 685 cm^{-1} respectively.

The C═O ring-in-plane and ring-out-of-plane bending (or C═O wagging and rocking) modes are known to occur in the range 650–690 cm^{-1} in some α,β-unsaturated esters[20]. The amorphous band at ~ 645 cm^{-1} is tentatively assigned to $\rho_{C=O}$ (ν_{17}) in PET and PCHT.

Finally, the C—(C═O) out-of-ring-plane bending mode (ν_{18}) has been assigned to the amorphous band at ~ 295 cm^{-1} in both polymers. In *p*-xylene, $\delta_{[C-(CH_3)\perp]}$ (B_{3g}) occurs at 313 cm^{-1}, and in terephthalic acid, weak absorption at 295 cm^{-1} is also attributed to this vibration.

B_{1u}, B_{2u} and B_{3u} species

All the '*B*' type species are infra-red active in both the V_h and C_{2v} configurations of the terephthalate framework. However, since the latter configuration implies a departure from planarity, this in turn will be associated with a loss of resonance of the C—C bonds and the intensities of many of the 'B_u' vibrational modes will be expected to increase slightly upon crystallization, accompanied by a slight frequency shift. Since the bands originate essentially in the crystalline planar V_h configuration they are denoted as being of crystalline origin. The 'amorphous' bands of the A_g, B_{2g} and B_{3g} species would, of course, be almost completely absent from highly crystalline specimens.

B_{1u} species

The B_{1u} vibrational modes in both PET and PCHT are expected to exhibit σ polarization with respect to the plane normal to the film. The $\delta_{[C-(C=O)+C-H]}$ out-of-ring-plane deformation mode (ν_{21}) is derived from ($\nu_{17}B, E_{2u}$) in benzene, and will lie at an appreciably lower frequency than $\nu_{17}B$, which occurs at 985 cm^{-1}. In *p*-xylene the vibration occurs[14] at 800 cm^{-1}. The strong σ absorption at 730 cm^{-1} in both polymers is consequently assigned to this vibration, which is believed to contribute the medium–strong absorption at ~ 730 cm^{-1} in all the model compounds studied.

The other $\delta_{[C-(C=O)+C-H]\perp}$ mode (ν_{24}) in this species is derived from (ν_{11}, A_{2u}) in benzene (671 cm^{-1}) and is expected at a very much lower frequency in para substituted derivatives. In *p*-xylene, the mode has been assigned[14] at 170 cm^{-1}. Therefore the mode is assigned to the weak absorption common to both polymers at 155 cm^{-1}. The absorption of amorphous origin at 875 cm^{-1} has been assigned[5] to ν_{21} and the σ band at 730 cm^{-1}

to ν_{24}. Since ν_{24} is expected to lie at a low frequency, from an examination of its normal form of vibration, it is unlikely that this mode in the para substituted ring could occur at a higher frequency than in the C_6H_6 molecule (671 cm^{-1}). In addition, no absorption at $\sim$ 870 cm^{-1} was noted in PCHT. We therefore prefer to assign the amorphous σ band at 875 cm^{-1} in PET, which on deuteration[5] shifts to 820 cm^{-1}, to ρCH_2 (ν'_{48}, A).

The ring-out-of-plane deformation mode, $\delta_{CCC\perp}$ (ν_{23}) is derived from ($\nu_{16}B$, E_{2u}) in benzene (400 cm^{-1}) and is expected to occur at a similar frequency in the two polymers. Weak absorption of σ polarization at $\sim$ 424 cm^{-1} is attributed to this mode.

Finally, the $\rho_{C=O}$ mode (ν_{22}) is assigned to weak absorption in both PET and PCHT at 515 cm^{-1} by analogy with some α,β-unsaturated esters[20].

B_{2u} species

All the B_{2u} modes derived from the benzene ring vibrations are expected to display π polarization; the $\nu_{as\,C=O}$ (ν_{26}) vibration will display σ dichroism. The latter mode is readily assigned to the intense σ absorption at $\sim$ 1 720 cm^{-1} in both polymers. The vibration gives rise to strong absorption in esters and carboxylic acids in the region 1 720–1 680 cm^{-1}.

The π absorption at $\sim$ 3 060 cm^{-1} in both polymers is assigned to the (ν_{sCH}) mode (ν_{25}) (which persists in most of the 'aromatic' model compounds examined). In para dideuterobenzene the mode is found[21,22] at 3 060 cm^{-1}, and is derived from ($\nu_{20}A$, B_{1u}) in benzene at 3 046 cm^{-1}.

ν_{CC} (ν_{27}) is derived from ($\nu_{19}A$, E_{1u}) (1 485 cm^{-1}) in benzene. The band shifts to $\sim$ 1 415 cm^{-1} on deuteration[5] and so a 'mixed' vibrational mode with some C—H motion is indicated. In *p*-xylene the mode is believed to occur at 1 525 cm^{-1}. The only suitable π absorption common to both polymers is at 1 498 cm^{-1}.

ν_{29}, $\delta_{CH\parallel}$, is derived from ($\nu_{18}A$, E_{1u}) in C_6H_6 (1 037 cm^{-1}) and since the para substituents do not move in this vibration the mode is readily assigned to the medium–strong π absorption at 1 015 cm^{-1} in PET and PCHT and related model compounds.

The C—(C=O) asymmetric stretching mode (ν_{28}) is expected to occur at a considerably lower frequency than the corresponding mode in C_6H_6 [ν_{13}, E_{1u} (3 080 cm^{-1})] and to show some double bond character due to resonance within the terephthalate framework. It therefore lies midway between a pure ν_{C-C} (1 000 cm^{-1}) and $\nu_{C=C}$ (1 600 cm^{-1}), i.e. $\sim$ 1 300 cm^{-1}. Of the π bands common to both polymers occurring in this region only the medium band of crystal origin at $\sim$ 1 335 cm^{-1} is appropriate, since the common π band at 1 370 cm^{-1} is of distinctly amorphous origin and the π bands at 1 266 and 1 402 cm^{-1} are known to be due to $\nu_{as\,C-O}^{\parallel}$ and δ_{COH} respectively. The extent of the possible shift of the 1 335 cm^{-1} band, if due to ω_{CH_2}, upon deuteration of the glycol residue is not clear since any shift to shorter wavelengths corresponding to ω_{CD_2} would be masked by the intense absorption at 1 266 cm^{-1}, due to $\nu_{C-O}^{\parallel}$. Even in the deuterated glycol derivative there is weak absorption at 1 340 cm^{-1} (ref. 7), and it is possible that ω_{CH_2} and $\nu_{C-(C=O)}$ are coincident.

The medium π absorption at 970 cm^{-1} in both polymers, which increases

slightly upon crystallization, may be due to ring in-plane deformation (ν_{36}). This band shifts very slightly upon deuteration of the glycol residue in PET[7]. The corresponding inactive mode in C_6H_6 (ν_{12}, B_{1u}) is believed to occur at 1 010 cm^{-1} and no significant shift is expected in the para substituted ring.

B_{3u} species

The B_{3u} modes are expected to show σ polarization with respect to the drawing axis in the film plane, except for $\nu_{as\,C=O}$ (ν_{35}) which is expected to show π polarization. In $\nu_{as\,CH}$ (ν_{31}) and $\delta_{CH\parallel}$ (ν_{34}) which are derived from ($\nu_{20}B$, E_{1u}) and ν_{15} (B_{2u}) respectively in C_6H_6, the para substituents do not move. ν_{31} is consequently expected to lie very close to $\nu_{20}B$ in C_6H_6. The mode occurs at 3 080 cm^{-1} in both C_6H_6 and *p*-xylene. The σ absorption at $\sim$3 090 cm^{-1} in PET and PCHT is therefore assigned to ν_{31}. The medium absorption at 1 170 cm^{-1} in PET and PCHT is assigned to ν_{34}, $\delta_{CH\parallel}$. In C_6H_6, the corresponding mode (ν_{15}, B_{2u}) occurs at 1 170 cm^{-1} and in terephthalic acid[19] at 1 180 cm^{-1}. The 1 170 cm^{-1} absorption in both polymers is surrounded by a complex of absorption bands and so its polarization is not well defined. An alternative assignment for this mode is that it is masked by the strong π absorption at $\sim$1 100 cm^{-1} due to $\nu_{(C-O)}$. Support for this assignment lies in the fact that terephthalic acid has weak absorption at 1 110 cm^{-1} which has been assigned[19] to $\delta_{CH\parallel}$ and this band could not be associated with $\nu_{(C-O)}$. The mode in *p*-xylene is believed[14] to occur at 1 100 cm^{-1}.

The assignments of the two ring modes, ν_{32} and ν_{33} pose some difficulty. In benzene the corresponding modes are known to occur at 1 693 cm^{-1} [calculated value for ν_{14} (B_{2u})] and 1 485 cm^{-1} ($\nu_{19}B$, E_{1u}). The latter occurs as a weak band in the infra-red. From the form of the normal vibrations the modes in the para substituted ring are expected to occur at similar frequencies to those in benzene. In *p*-xylene, ν_{33} occurs weakly at 1 450 cm^{-1}. The only σ absorption common to both polymers in this region is at 1 460 cm^{-1} and this absorption is consequently assigned to ν_{CC}. In terephthalic acid the mode is assigned at 1 458 cm^{-1}. However, the absorption in the two polymers at $\sim$1 460 cm^{-1} is also undoubtedly contributed to by δ_{CH_2} of the glycol fragment in PET [in ethylene glycol δ_{CH_2} (B) = 1 459 cm^{-1}] and by δ_{CH_2} in the 1,4-cyclohexane dimethanol fragment in PCHT (δ_{CH_2} = 1 452 cm^{-1}). Since these δ_{CH_2} modes are also expected to exhibit σ polarization the assignment of neither ν_{CC} (ν_{33}) nor δ_{CH_2} (B) can be made with certainty.

The other ring mode (ν_{32}) corresponding to ν_{14} (B_{2u}) in C_6H_6 is attributed to the 1 515 cm^{-1} band. (The calculated value of the inactive mode in benzene is 1 693 cm^{-1}.) In terephthalic acid, a band at 1 510 cm^{-1} has been attributed to a ring stretching mode[19]. In PET and PCHT common absorption at 1 613 cm^{-1} and 1 515 cm^{-1} was noted, all other common unassigned bands in the region 1 400–1 700 cm^{-1} being of π polarization. The 1 613 cm^{-1} band has already been assigned to $\nu_{s\,C=O}$ (A_g).

ν_{36} involves only the in-ring-plane bending of the para substituent C—(C=O) group about the para axis and is expected to lie in the far infra-

red region. In *p*-xylene the mode has been assigned[14] at 232 cm^{-1} and in terephthalic acid the mode is thought to occur at 225 or 240 cm^{-1}. Consequently, the weak σ bands observed in the infra-red spectra of both polymers at ~ 235 cm^{-1} are assigned to $\delta_{C-(C=O)\parallel}$.

Finally, the π absorption in both polymers at ~ 630 cm^{-1} is assigned to ν_{35}, $\omega_{C=O}$. In acrylic and methacrylic esters[20] $\omega_{C=O}$ occurs at ~ 650 cm^{-1}. The assignment of the 630 cm^{-1} band as a combination tone[5] is rejected since the absorption persists in all the terephthalate model compounds studied, and in isophthalates the band appears to shift to 656 cm^{-1}, and is not shifted significantly on ring deuteration.

THE NORMAL MODES OF VIBRATION OF THE FRAGMENT [—O—CH_2CH_2—O—]

In predicting the spectrum of the glycol residue it will be assumed that in highly oriented crystalline PET a *trans* configuration is predominant, and in amorphous regions both *trans* and *gauche* configurations exist. Previous spectral measurements on PET can indeed only be satisfactorily explained on the basis of such a rotational isomerism[1-4]. Comparison of the spectra of PET with PCHT clearly show that many bands in PET not found in PCHT, and therefore likely to be due to the glycol residue, are of definite crystalline or amorphous origin. A normal coordinate analysis of the fragment [—C—O—CH_2CH_2—O—C—] in PET for both *trans* and *gauche* configurations[23] has produced a set of frequency values for the normal modes of each symmetry type consistent with the spectral results for the 'glycol' bands obtained for amorphous and crystalline PET in this investigation.

'Trans' configuration

The glycol fragment of *trans* configuration will possess the symmetry C_{2h} and will contribute $(3N-6)$ or 18 normal modes of vibration which, according to *Table 3*, will divide as follows:

$$5A_g + 4B_g + 4A_u + 5B_u$$

where the A_g and B_g species are Raman active, and the A_u and B_u species are infra-red active. The numbering and approximate description of the 18 normal modes is given in *Table 11*.

'Gauche' configuration

The *gauche* fragment, believed to exist predominantly in amorphous regions of PET, will possess the symmetry C_2 and, according to *Table 4*, the 18 normal modes will then divide as follows:

$$10A + 8B$$

where both the A and B species are active in the Raman and infra-red effects. The correlations between the corresponding modes of the C_{2h} and C_2 symmetry species is given in *Table 11* together with a description of the

Table 11. Observed and calculated frequencies for the vibrational modes in *trans* and *gauche* —O—CH_2—CH_2—O— fragments in PET and in ethylene glycol

Trans (C_{2h}) [$C_{2v}(Z)$] *species*	*No.*	P	ν_i (*obsd*)	ν_i‡ (*calc.*)	*Gauche*† [$C_2(y)$] *species*	*No.*	P	(*obsd*)	(*calc.*)	*Ethylene glycol gauche* (*obsd*)	*Assignment*
A_g	37	—	—	—	*A*	37′	π	2882	2853	2875	$\nu_{s\,CH_2}$
	38	—	—	—	*B*	38′	π	1435	1487	1459	δ_{CH_2}
	39	—	—	—	*A*	39′	σ	1335	1356	1332	ω_{CH_2}
R	40	—	—	—	*A*	40′	π	1041	1214	1038	$\nu_{s\,CO}$
(*P*)	41	—	—	—	*A*	41′	π	869	1171	864	ν_{CC}
B_g	42	—	—	—	*A*	42′	π	2959	2905	2935	$\nu_{as\,CH_2}$
	43	—	—	—	*A*	43′		1200	1047	1212	τ_{CH_2}
R	44	—	—	—	*B*	44′	π	939	973	1061	ρ_{CH_2}
(*dp*)	45	—	—	—	*A*	45′		117	—	—	τ_{OCCO}
A_u	46	π	2907	2940	*B*	46′	π	2967	2908	2938	$\nu_{as\,CH_2}$
	47		1100	1108	*B*	47′		1260	1258	1260	τ_{CH_2}
IR	48	π	852	900	*A*	48′	π	893	892	887	ρ_{CH_2}
	49	σ	306	—	—			—	—	—	$\delta_{CCO\perp}$
			—	—	*B*	49′	σ	345	340	352	$\delta_{CCO\parallel}$
B_u	50	π	2852	2850	*B*	50′	π	2890	2860	2875	$\nu_{s\,CH_2}$
	51	π	1468	1510	*A*	51′	π	1448	1500	1459	δ_{CH_2}
	52	σ	1335	1330	*B*	52′	σ	1377	1355	(1370)*	ω_{CH_2}
IR	53	π	1120	1100	*B*	53′	π	1100	1096	1087	$\nu_{as\,CO}$
	54	π	504	500	*A*	54′	π	434	425	478	$\delta_{CCO\parallel}$

* Only observed in DO—CH_2CH_2—OD.

† The *A* and *B* species of C_2 symmetry are both active in the infra-red (IR) and Raman (R) effects.

P Predicted infra-red dichroism in oriented polymer.

‡ Ref. 24.

approximate modes of vibration involved. Due to the different twofold rotation axes in the C_{2h} and C_2 symmetry forms there is a 'mixed' correlation between the species of each symmetry. In addition, the CCO out-of-plane bending mode ν_{48} (A_u) in the *trans* form becomes a non-genuine vibration (rotation) in the *gauche* form, whilst the CCO in-plane bending mode [ν'_{49} (B)] in the *gauche* form becomes a non-genuine vibration (rotation) in the *trans* form. These 'non-genuine' vibrations $\delta_{CCO\parallel}$ (*trans*) and $\delta_{CCO\perp}$ (*gauche*), become the hindered skeletal torsional modes about the O—CH_2 bond (τCOCC), which are the modes ν_{59} (A_g) and ν'_{59} (B) in the *trans* and *gauche* configurations of the polyester, respectively. All other modes of vibration in the C_{2h} isomer are found to be of similar origin to those in the C_2 isomer.

The numbering of the normal vibrations in the glycol residue in *Table 11* is therefore based on the grouping of the normal modes in the C_{2h} configuration (unprimed frequencies). The modes of the C_2 configuration, corresponding approximately in motion to those in the C_{2h} form, are primed. The frequency notation of the glycol residue follows on that of the terephthalate framework. Consequently the 18 'glycol' modes in the polymer repeat unit are numbered ν_{37}–ν_{54} for the *trans* configuration and ν'_{37}–ν'_{54} for the *gauche* configuration.

The origin of the so-called 'crystalline' and 'amorphous' bands due to rotational isomerism of the glycol fragment is now apparent. The A_g and B_g modes of the *trans* C_{2h} form will be inactive in the infra-red and therefore absent from highly crystalline specimens. However, the corresponding A and B modes of the *gauche* C_2 form will appear strongly in amorphous regions of the polymer due to the change in selection rules. In PET specimens of low crystallinity the infra-red spectrum will be complicated by the presence of the active A_u and B_u crystalline *trans* modes and by the corresponding active A and B modes of the *gauche* form which are expected to display significant frequency shifts from the corresponding *trans* modes.

ASSIGNMENT OF THE NORMAL MODES OF THE FRAGMENT [—O—CH_2—CH_2—O—]

The results of Sawodny *et al.*[24] show no evidence for the existence of C_{2h} symmetry in ethylene glycol, since almost all Raman lines have infra-red counterparts which is contrary to the mutual exclusion rule applicable to C_{2h} symmetry. Consequently their assignments are based on a C_2 model in consonance with Kanbayashi and Nakuda[25] who studied the solvent and temperature dependence of the vibrational bands of ethylene glycol and concluded that only the *gauche* configuration is present in all states of the compound. The calculation of the vibrational frequencies of the *trans* and *gauche* configurations of the glycol fragment in PET[23] is also of interest. In the analysis a set of force constants was used which was obtained from the spectral data for low molecular weight compounds. The results of the analysis are summarized in *Table 11* together with the observed values. As the spectrum analysis of the previous section indicated, the calculated frequencies for the corresponding vibrational modes in the C_{2h} (*trans*) and

C_2 (*gauche*) configurations differ significantly. Also summarized in *Table 11* are the assignments for the *gauche* ethylene glycol molecule, included for comparison. The overall agreement between observed and calculated frequencies is satisfactory.

CH_2 *modes*

The assignments of the CH_2 modes in the glycol residue have already been discussed in some detail by previous workers, and are summarized along with the calculated values[23] in *Table 11*. Consequently the discussion will be limited to the assignments of the CH_2 twisting and rocking modes.

CH_2 *twisting modes*—The CH_2 twisting vibrations are expected to be weak and to lie at slightly lower frequencies than the CH_2 wagging modes. Due to the forms of these vibrations, their dichroism is not expected to be of any aid in their identification.

A thorough examination of the spectral data reveals that no definite assignments can be made for any of the CH_2 twisting modes. In the *trans* crystal spectrum a band due to τ_{CH_2} [ν_{47} (A_u)] is predicted at 1 108 cm^{-1} but is most probably completely masked by the intense absorption at 1 100 cm^{-1}, due to $\nu_{as\,C-O}$. Likewise the 'amorphous' τ_{CH_2} modes predicted at 1 258 [ν'_{47} (B)] and 1 047 cm^{-1} [ν'_{43} (A)] are probably masked by the strong absorptions at 1 266 cm^{-1} and 1 041 cm^{-1} which are due to skeletal —C(=O)—O— stretching and $\nu_{s\,C-O}$ [ν'_{40} (A)] respectively.

CH_2 *rocking modes*—Due to the uncertainty in the spatial orientation of the —OCH_2CH_2O— grouping with respect to the fibre axis in oriented PET the dichroisms of the rocking modes are especially difficult to predict; they may well be different in the C_{2h} and C_2 configurations. Absorption due to CH_2 rocking in short-chain hydrocarbons is expected in the region of 800 cm^{-1}. However, the out-of-phase CH_2 rocking frequency in the C_2 form, ν'_{44} (B) is calculated[23] to be at 973 cm^{-1}. In ethylene glycol absorption at 1 061 cm^{-1} has been attributed to this mode[24]. We have failed to observe absorption appropriate to such an 'amorphous' rocking mode ν'_{44} (B) in the region of 1 060 or 970 cm^{-1} and conclude that the absorption is weak and probably masked by other strong absorptions in these regions. A very weak band is observed only in amorphous PET at 939 cm^{-1} but is too low to be consistent with the predicted frequency, and with that observed in ethylene glycol.

The in-phase CH_2 rocking mode ν_{48}, is expected to be more intense and to occur at a lower frequency than $\rho_{as\,CH_2}$. (ν'_{44}), the amorphous π band at 893 cm^{-1} is assigned to ρ_s [ν'_{48} (A)] and compares favourably with the calculated value of 892 cm^{-1} and the corresponding mode observed in ethylene glycol[24] at 887 cm^{-1}. The strong crystal π band at 852 cm^{-1} is assigned to the A_u *trans* rocking mode (ν_{48}). The predicted frequency for this vibration is 900 cm^{-1}. This band disappears completely in the spectrum of the molten polymer[8].

It has been suggested[6] that in poly(ethylene glycol) the strong bands occurring at 1 470 cm^{-1} (δ_{CH_2}), 1 344 cm^{-1} (ω_{CH_2}) and 844 cm^{-1} (ρ_{CH_2}) are associated with a *gauche* configuration of the —OCH_2CH_2O— group. These results are in contrast with those obtained[24] for HO—CH_2CH_2—OH and

DO—CH_2CH_2—OD in which the strong absorptions associated with their *gauche* configurations[25] occur at 1 459 cm^{-1} (δ_{CH_2}), 1 370 cm^{-1} (ω_{CH_2}), and 887 cm^{-1} (ρ_{CH_2}). These bands appear only weakly in the spectrum of poly(ethylene glycol). The correlations between the spectra of poly(ethylene glycol) and crystalline PET have been made the basis of a possible *gauche* configuration for the ethylene glycol residue in the latter[6], thus explaining the observed polarizations of the ν_{sCH_2} and ν_{asCH_2} modes, which are opposite to those predicted on the basis of Bunn's essentially planar PET structure[11]. However, it is likely that in the PET crystal the single molecule contained in the triclinic cell will be potentially centrosymmetric[11], thus favouring a *trans* configuration of the glycol residue. The unexpected dichroisms of ν_{sCH_2} and ν_{asCH_2} must then arise due to rotation about the O—CH_2 and phenylene–carbonyl bonds additional to that implied by the PET crystal structure analysis[11], and in such a way that the centre of symmetry of the unit cell is preserved.

SKELETAL MODES

—C—O— *stretching modes*

Absorption due to stretching of the C—O bonds generally occurs in the region 1 000–1 300 cm^{-1}. In esters C—O bond stretching which is relatively unaffected by resonance absorbs near 1 100 cm^{-1}, whilst the 'stiffer' —$\overset{\|}{C}$—O— bond stretching frequency is raised to $\sim$1 300 cm^{-1} due to resonance. The strong infra-red absorption of π polarization in PET at 1 266, 1 120, 1 100 and 1 041 cm^{-1} is consequently attributed to C—O bond stretching in the glycol–ester linkage. The very intense 1 266 cm^{-1} band is attributed to —C—O— bond stretching (ν_{60}). Tadokoro[8] has observed that the intensity of the 1 041 cm^{-1} band is considerably diminished in the spectrum of molten PET.

The intense π band at 1 100 cm^{-1} is partly attributed to ν_{asC-O} (*B*) [ν'_{53}] in the *gauche* configuration. This band was designated[5] as of amorphous origin but no significant decrease in intensity with increasing crystallization was detected. This band is predicted[23] to occur at 1 096 cm^{-1}. In ethylene glycol the mode is assigned[24] to strong absorption at 1 087 cm^{-1}. No other absorption was observed in this region in ethylene glycol.

The assignment of the two bands at 1 100 and 1 120 cm^{-1} in PET to the proposed C_{2h} and C_2 configurations of the glycol fragment does not then in this instance imply that they are due entirely to a difference in configuration between the two methylene groups between the two symmetry forms but rather to the relative change in configuration of each symmetry form with respect to the terephthalate framework. This could be brought about by rotation of each glycol fragment about the —O—CH_2— and —$\overset{\|}{C}$—O— bonds. This hypothesis is borne out by the appearance of the two similar bands in PCHT which could not arise as a result of rotational isomerism of adjacent methylene groups. The other vibrations primarily affected by such rotation would be the in-plane and out-of-plane —$\overset{\|}{C}$—O—C—, C$\overset{\|}{C}$O and —O—C—C— deformation modes. These will be considered shortly.

The CH_2 vibrations in the glycol residue, although unaffected in frequency by such rotation about the O—CH_2 bonds, due to negligible coupling effects, would undergo a change in orientation with respect to the fibre axis and hence a change in dichroism. This might be a possible explanation of the inconsistencies observed in the polarization of many of the CH_2 modes from those predicted for the 'rigid' crystalline model of Bunn *et al.*, which structure may be in error with respect to the orientation of the CH_2 groups. The location of these carbon atoms was the least reliable part of their structure determination[11]. Such rotation occurs in other polymers as is shown by the large rotation about the O—CH_2 bond observed in poly(ethylene adipate)[11,26].

The absorption of amorphous origin at 1 041 cm^{-1} is attributed to in-phase ν_{sC-O} [ν'_{40} (A)]. In ethylene glycol the mode is assigned[24] at 1 038 cm^{-1}. The marked disagreement between the observed (1 041 cm^{-1}) and calculated (1 270 cm^{-1}) frequency values probably arises because in the calculation the interaction between the atoms at the end of the glycol fragment and the rest of the chain was ignored[23]. Also, the calculation does not take into account the proposed rotation about the —OCH_2 and —C—O— bonds, which would have a significant effect on ν_{sC-O}, ν_{asC-O}, $\delta_{CCO\perp}$ and $\delta_{CCO\parallel}$.

C—C *stretching*

The C—C stretching vibration in the glycol fragment is expected to show π polarization in the region 900–1 000 cm^{-1}, where it is known to occur in short-chain aliphatic ketones and aldehydes. The only band that can be reasonably assigned to ν_{CC} in ethylene glycol[24] is a medium band at 864 cm^{-1}. Consequently the amorphous band at 869 cm^{-1} in PET is assigned to ν_{CC} [ν'_{41} (A)]. The corresponding *trans* band ν_{41} (A_g) is forbidden by the selection rules for C_{2h} symmetry. The predicted frequency[23] for ν_{CC} (A) is 1 171 cm^{-1}, which is clearly far from agreement with the assigned frequency, 869 cm^{-1}. In spite of this the assignment of ν_{CC} (A) to 869 cm^{-1} is preferred since no corresponding absorption of the appropriate polarization or amorphous origin was detected in PCHT. Absorption was, however, noted in PET and PCHT at $\sim$ 1 175 cm^{-1}, and is attributed to $\delta_{CH\parallel}$ in the terephthalate framework. No absorption in the region of 1 170 cm^{-1} was observed in ethylene glycol. It is felt that the calculated value for ν_{CC} (ν_{41}) in PET is too high due to neglect of significant skeletal interaction terms in the potential function, and to neglect of the rotation about the —OCH_2 and C—O bonds. The overall agreement between the observed and calculated CH_2 modes is, however, satisfactory. Little coupling is, of course, expected between the CH_2 modes and the chain skeleton outside the glycol fragment.

CCO *bending modes*

The two in-plane CCO bending modes in ethylene glycol have been assigned[24] at 478 cm^{-1} (A) and 352 cm^{-1} (B) respectively. Consequently in PET the π band at 434 cm^{-1} is assigned to $\delta_{CCO\parallel}$, ν'_{54} (A) and the broad σ band (of definite amorphous origin) at 345 cm^{-1} is assigned to $\delta_{CCO\parallel}$, [ν'_{49} (B)]. The predicted values of the corresponding modes in the *gauche*

glycol fragment [ν'_{54} (A) and ν'_{49} (B)] are 425 cm^{-1} (π) and 340 cm^{-1} (σ) respectively (the assumption being made that the latter vibrations are not greatly affected by the neglect of skeletal interaction terms).

The mode corresponding to $\delta_{CCO_{\parallel}}$ in the *trans* crystal configuration (ν_{54}) is predicted[20] to occur at 500 cm^{-1} (π). The only band which can be reasonably assigned to this mode in PET is the 'crystal' π band at 504 cm^{-1}.

The $\delta_{CCO_{\perp}}$ bending mode [$\nu_{49}\, A_u$] peculiar to the *trans* configuration is tentatively assigned to the weaker π band at 306 cm^{-1}. Similar absorption at 313 cm^{-1} is observed in 1,6-hexanediol dibenzoate.

We have not been able to detect the absorption due to torsion about the OCCO bond in ethylene glycol, but expect it to lie in the region of 250 cm^{-1}.

THE 'INTERNAL' STRETCHING, DEFORMATION AND TORSIONAL MODES OF THE CHAIN SKELETON

The PET repeat unit will possess ($3N-4$), i.e. 62, fundamental modes of vibration. The terephthalate ring framework —OC . C_6H_4 . CO— contributes 36 normal vibrations (+6 non-genuine vibrations) and the ethylene glycol fragment —O—CH_2—CH_2—O— contributes 18 normal vibrations (+6 non-genuine vibrations). Consequently, of the 12 'null' modes predicted for the two 'discrete' fragments ($62-54$), i.e. eight of these vibrations will become internal skeletal modes when the two fragments join to form the repeat unit. These internal skeletal modes will result in a skeletal stretching vibration involving essentially stretching of the —O—C(=O)— bond, $\nu_{(O-\overset{\|}{C}O)}$, four 'chain bending' modes involving essentially —C(=O)—O—C and C—C(=O)—O in-plane bending and —C(=O)—O—C and —C—C(=O)—O out-of-plane bending, and three skeletal torsional modes. The latter will arise due to rotation about the three bonds.

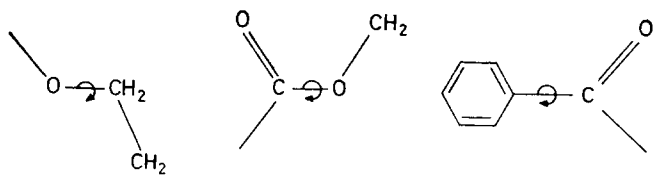

and these are designated τCCOC, τCCOC, and $\tau(C_6H_4)CO$ respectively.

The symmetries of these normal skeletal modes must be considered under the appropriate factor group or unit cell group which, for the *trans* configuration of the glycol fragment and the planar terephthalate framework on the basis of Bunn's structure[11], will be C_i. For the *gauche* configuration of the glycol fragment, taken in conjunction with the non-planar terephthalate framework, the unit cell group in PET will be C_2 [$C_2(y)$].

It should be noted that the exact forms of the skeletal vibrations are not known, but in the *trans* C_i form they can be designated as being either symmetric (A_g) or antisymmetric (A_u) with respect to the appropriate centre of inversion; for the *gauche* form of C_2 symmetry they may be symmetric

Table 12. Assignment of the 'internal' skeletal modes in poly(ethylene terephthalate)

Unit cell group C_i trans†	*No.*	ν_i	P	*Unit cell group C_2 gauche*‡	*No.*	ν_i	P	*Assignment*
A_g	55	458	π	*A*	55′	289	π	$\delta_{CCO\parallel}^{\parallel}$
A_g	56	177	π	*A*	56′	190 [162]*	π	$\delta_{COC\parallel}^{\parallel}$
A_g	57	95	π	*B*	57′	117	π	$\tau_{(C_6H_4)CO}^{\parallel}$
A_g	58	—		*B*	58′	70	σ	$\tau_{CCOC}^{\parallel}$
A_g	59	62	σ	*B*	59′	46		$\tau_{COCC}^{\parallel}$
A_u	60	1266 [1325]	π	*B*	60′	1248 [1270]	π	$\nu_{(-C-O-)}^{\parallel}$
A_u	61	379 [330]	π	*B*	61′	423/417 [430]	π	$\delta_{COC\perp}^{\parallel}$
A_u	62	139	π	*B*	62′	274/260		$\delta_{CCO\perp}^{\parallel}$

* Calculated frequencies are given in parentheses.

† The C_i *trans* modes are expected to have crystal origin.

‡ The C_2 *gauche* modes are expected to have amorphous origin.

P Predicted infra-red dichroism in oriented polymer.

(*A*) or antisymmetric (*B*) with respect to the C_2 (*y*) axis (*Table 12*). The *y* axis is taken to be the axis perpendicular to the chain axis in the plane of the benzene ring.

In this manner, the eight internal skeletal vibrations are found to divide, under the C_i unit cell group, as follows:

$$5A_g + 3A_u$$

the A_g modes being Raman active and the A_u modes infra-red active.

Similarly, under the C_2 unit cell group, the eight internal skeletal modes will divide as follows:

$$2A + 6B$$

where the *A* and *B* modes are both Raman and infra-red active. The correlations between the corresponding modes of the postulated C_i and C_2 symmetry forms are given in *Table 12*, together with approximate descriptions of the motions involved. It is reasonable to predict that significant differences will occur between absorption frequencies of the corresponding vibrations in the two proposed configurations, since the 'equilibrium' spatial orientation of the glycol fragment in the C_i form with respect to the terephthalate framework will be quite different to that in the C_2 form. This effect will be brought about by the additional 'rigid' rotation of the *trans* and *gauche* glycol fragments about the O—CH_2 and —C—O— bonds in the respective symmetry forms. Consequently, it ought to be possible to observe frequency shifts in all the internal skeletal modes due to the different molecular environments, and to steric hindrance, which should affect the torsional modes.

Although all the A_g skeletal modes of the C_i unit cell group symmetry are theoretically infra-red inactive, they are expected to show weak infra-red activity. This would come about when any two equivalent fragments or groups in the polymer repeat unit are no longer strictly related by a centre of symmetry. The factor or unit cell group gives only an indication of the activity of the internal skeletal modes in a highly ordered crystal. It is probably the local symmetry of the fragment undergoing the vibration that governs the infra-red activity[5] and even in a highly ordered PET crystal it is probable that, with such a complex molecular geometry, rotation about the O—CH_2 and C—O bonds, together with crystal field effects, will invalidate the selection rules.

—C(=O)—O— SKELETAL STRETCHING MODES

In most esters the —C(=O)—O— bond stretching mode absorbs strongly in the infra-red in the region of 1 300 cm^{-1}. Consequently, the intense π absorption at 1 266 cm^{-1} is attributed to $\nu_{(C-O)}^{\|}$ in PET. This band does increase slightly in intensity in heat-treated samples and is thought to have some crystal origin. According to *Table 12* two infra-red active C(=O)—O stretching

modes are predicted for the two postulated configurations of PET—one of definite crystal origin (C_1 form) and the other of amorphous origin (C_2 form). Both modes are expected to display parallel dichroism. The 'shoulder' band at 1 248 cm^{-1}, which shows π polarization, is found to diminish in intensity upon drawing and heat treatment.

Values of 1 325 (π) and 1 270 (π) have been calculated for $\nu^{\parallel}_{C-O}$ (*trans*) and $\nu^{\parallel}_{C-O}$ (*gauche*) respectively[23] in the PET glycol fragment. In terephthalic acid $\nu^{\parallel}_{C-O}$ occurs at 1 282 cm^{-1}. The infra-red absorption[5] at 1 266 cm^{-1} (c, π) and 1 248 cm^{-1} (a, π) are therefore assigned to ν_{60} (A_u) and ν'_{60} (B), for the C_1 and C_2 configurations, respectively.

ASSIGNMENT OF THE CCO AND COC 'INTERNAL' SKELETAL DEFORMATION MODES

According to *Table 12* there are four internal skeletal deformation modes expected for the *trans* and *gauche* configurations of the PET repeat unit. These are designated $\delta^{\parallel}_{COO\parallel}$, $\delta^{\parallel}_{COC\parallel}$, $\delta^{\parallel}_{COO\perp}$, and $\delta^{\parallel}_{COC\perp}$, where $\parallel$ and $\perp$ denote deformations occurring essentially in the plane of the benzene ring, and out of the benzene ring plane respectively, in fully oriented, extended polymer. Since the configuration of the COC linkage in both forms will be quite different, the frequencies of the corresponding modes in each form are expected to differ significantly.

Since the exact form of these normal vibrations is not known it is difficult to make definite assignments or to predict the infra-red dichroism for these vibrations. It might be expected that such vibrational modes would exhibit σ polarization but since the forms of these vibrations are sensitive functions of the masses[5], for certain mass distributions the modes will exhibit π polarization, as in CH_3COCH_3[27].

The $\delta^{\parallel}_{COC\perp}$ mode is calculated to be at 330 cm^{-1} (ν_{61}) in the *trans* polyester, and at 430 cm^{-1} (ν'_{61}) in the *gauche*[23]. A strong crystal band at 379 cm^{-1} is accordingly assigned to ν_{61} (A_u, *trans*) and the weak amorphous band at 417 cm^{-1} is attributed to ν'_{61} (B, *gauche*). The $\delta^{\parallel}_{CCO\perp}$ (A_u) mode is assigned to the π band at 139 cm^{-1} in highly crystalline PET. This band is almost totally absent from amorphous polymer. These assignments are consistent with the spectral behaviour of the 379 and 139 cm^{-1} absorptions, since both ν_{61} and ν_{62} are expected to be infra-red active modes in the crystal, appearing much more strongly in the crystal than the 'in-plane' counterparts of the A_g species which appear due to a breakdown in selection rules. In 1,6-hexanediol dibenzoate a medium crystal band at 136 cm^{-1} is attributed to $\delta^{\parallel}_{CCO}$ (ν_{62}, A_u in PET). The *gauche* counterpart of ν_{62}, viz. ν'_{62} is tentatively assigned to the weak absorption of amorphous origin at 260–274 cm^{-1}.

The prediction[23] for $\delta^{\parallel}_{COC\parallel}$ (ν'_{56}, A) in the *gauche* configuration is 162 cm^{-1}. This mode therefore seems to be the medium absorption of amorphous origin at 190 cm^{-1}. The *trans* counterpart (ν_{56}, A_g) is believed to be the weak absorption observed only in the crystal at 177 cm^{-1}. This absorption was observed only in crystalline ethylene glycol terephthalate monomer

and highly crystalline samples of ethylene glycol dibenzoate and 1,6-hexanediol dibenzoate.

The remaining modes, $\delta_{CCO_{\parallel}}^{\parallel}$, ν_{55} (A_g) and ν'_{55} (A) are expected to lie in the region 500–300 cm^{-1} and it is believed that the very weak crystal absorption at 458/474 cm^{-1} and the weak π absorption of amorphous origin at $\sim$290 cm^{-1} are probably attributable to these modes. Weak absorption does occur at these frequencies in most of the model compounds studied, including terephthalic acid. In the absence of a thorough coordinate analysis treatment of the terephthalate framework, however, the assignment of the δ_{CCO} skeletal modes must remain tentative. Of the four skeletal deformation modes assigned in PET (eight frequencies in all) only one occurs at a similar frequency and exhibits the same polarization band as that occurring in PCHT, namely the band of crystal origin at 177 cm^{-1}. The crystal origin of this band in PCHT is doubtful since its intensity scarcely varies upon crystallization and drawing. The far infra-red spectrum of PCHT contains far fewer bands of definite crystal origin compared to the PET spectrum, thus lending support for the purported existence of the discrete *trans* and *gauche* forms in PET.

SKELETAL TORSIONAL MODES

Most of the infra-red absorptions in PET below 130 cm^{-1} are expected to be due to skeletal torsion vibrations which are the only fundamental modes in PET likely to lie at such low frequencies. According to *Table 12* three torsional modes $\tau_{(C_6H_4)\overset{\parallel}{C}O}$, $\tau_{C\overset{\parallel}{C}OC}$ and $\tau_{COC\overset{\parallel}{C}}$ are expected to appear in the far infra-red for each of the two proposed configurations of the polymer repeat unit. The three torsional modes of the 'C_2' form are infra-red active and are expected to have amorphous origin. The three τ modes for the 'C_i' form, although infra-red inactive under the factor group C_i, may appear weakly in oriented, crystalline PET.

The highest-frequency torsional vibration is expected to be that due to 'hindered' rotation of the phenyl group about the chain axis, $\tau_{(C_6H_4)\overset{\parallel}{C}O}$ with the phenyl–carbonyl linkage as the rotation axis. The torsion about the phenyl–aldehyde bond in benzaldehyde has been assigned[28,29] at 111 cm^{-1} (vapour) or 133 cm^{-1} (liquid). In terephthalic acid, the lowest fundamental expected is the phenyl–carboxyl torsion and the absorption at $\sim$110 cm^{-1} is consequently attributed to this mode. In monomeric and oligomeric ethylene glycol terephthalate similar absorption is observed at 115 cm^{-1}, and in ethylene glycol dibenzoate the band shifts to 117 cm^{-1}. In amorphous PET broad, weak absorption occurs at 117 cm^{-1}, with a shoulder at $\sim$95 cm^{-1}. Upon drawing and subsequent crystallization by heat treatment the 117 cm^{-1} absorption in PET decreases sharply in intensity and is just detected at 108 cm^{-1} (π) in uniaxially oriented heat crystallized polymer, whilst the 95 cm^{-1} (π) band increases in intensity with increasing orientation and crystallinity. It is therefore suggested that the 'crystal' band at 95 cm^{-1} and the amorphous band at 117 cm^{-1} are due to the phenyl–carboxyl torsions, $\tau_{(C_6H_4)\overset{\parallel}{C}O}$, of the C_i (ν_{57}) and C_2 (ν'_{57}) configurations in PET. In ethylene glycol dibenzoate absorption of 'crystal' origin was ob-

served at 93 cm^{-1}, and in bis-β hydroxy ethyl terephthalate the absorption was noted at ~ 100 cm^{-1}. In 1,6-hexanediol dibenzoate pronounced absorption occurred at 123 and 87 cm^{-1}.

Further support for the above assignments for $\tau^{\parallel}_{(C_6H_4)CO}$ is the appearance of similar absorption of π polarization at ~ 115 cm^{-1} in *cis* and *trans* PCHT. Similar absorption was observed in all the model compounds containing terephthalic acid and 1,4-cyclohexanedimethanol fragments. However, the 'crystal' absorption at 93 cm^{-1} observed in PET was not present in PCHT. Since the $(C_6H_4)\overset{\|}{C}O$ torsion is taking place about the fibre axis in highly uniaxially oriented PET, the observed polarization of the 117 and 93 cm^{-1} bands in PET and the 115 cm^{-1} band in PCHT is not inconsistent with Bunn's PET crystal structure[11].

The lowest torsional mode in PET is expected to be due to the 'hindered' rotation about the —O—CH_2— axis, $\tau^{\parallel}_{OCCC}$, which is known to occur appreciably in a number of related long-chain molecules[11,26]. An absorption in amorphous PET at ~ 30 cm^{-1} was so weak as to raise doubts whether it was genuine. However, a definite 'doubtlet' was observed in amorphous PET, the stronger component lying at 45 cm^{-1} and the weaker at 58 cm^{-1}. Upon drawing and heat-induced crystallization the 46 cm^{-1} (π) band virtually disappeared, but the 58 cm^{-1} (σ) component slightly increased in intensity and shifted to ~ 62 cm^{-1} (*Figure 1*). This is explained on the basis of the postulated C_i and C_2 configurations since corresponding 'crystal' and 'amorphous' components for $\tau^{\parallel}_{OCCC}$ are predicted for each configuration (*Table 12*). As previously explained these two torsional vibrations originate from the 'non-genuine' vibrations in the glycol fragment, arising from in-plane CCO bending of the glycol residue of *trans* configuration (ν'_{49}) and the out-of-plane CCO bending of the glycol fragment of *gauche* configuration (ν_{49}). Consequently, the 'crystal' and 'amorphous' absorptions at 62 and 46 cm^{-1} are assigned to ν_{59} (C_i) and ν'_{59} (C_2). The behaviour of these bands, and the higher frequency of the 'crystal' torsional mode would appear to confirm the presence of a greater hindrance to internal rotation of the *trans* glycol fragment about the —O—CH_2— bond due to steric and crystal field effects. The assignment, if correct, would also confirm the relative ease with which such rotation could occur in both configurations, and thereby lend support for the occurrence of this rotation to be responsible for the disagreement in dichroism observed for the CH_2 groups in the ethylene glycol fragment, from those predicted on the basis of Bunn's postulated structure[11] where such rotation is not taken into account.

Since it is not known exactly to what extent the rotation about the —O—CH_2— and $-\overset{\|}{C}-O-$ bonds 'additional' to that postulated in the Bunn structure occurs, the dichroism of the torsional modes $\tau^{\parallel}_{CCOO}$ and $\tau^{\parallel}_{OCCO}$ for the postulated C_i and C_2 configurations of PET cannot be predicted with certainty. However, on the basis of the assignments just made for $\tau^{\parallel}_{OCCO}$, the 'crystal' C_i mode exhibits σ polarization and the 'amorphous' C_2 mode π polarization with respect to the fibre axis and the plane of the terephthalate framework. This would indicate a distinctly different spatial

orientation of the *trans* glycol fragment to that of the *gauche* form with respect to both the terephthalate framework and the fibre axis, lending further support for the existence of these two forms in PET. In ethylene glycol dibenzoate very weak absorption attributed to the $\tau^{\parallel}_{\text{COCC}}$ modes ν_{59} and ν'_{59} in PET was observed at 59 and 48 cm^{-1}. In 1,6-hexanediol dibenzoate absorption occurred at 60 and 46 cm^{-1}. Similar absorption displaying the same dichroism and intensity changes on crystallization was not observed in PCHT.

According to *Table 12*, one further skeletal torsional mode involving hindered rotation of the glycol fragment about the —C(=O)—O— linkage is predicted. This mode is assigned to infra-red absorption at ~ 70 cm^{-1}, the lowest absorption observed and as yet unaccounted for. Weak absorption was observed in the amorphous polymer at 68 cm^{-1} which hardly altered in intensity upon uniaxial drawing. After heat treatment the band weakened in intensity and displayed σ polarization. This torsional vibration corresponds to the 'free' rotation, R_y, of species B_{2g} of the discrete planar terephthalate framework about the y axis. In the polymer such rotation results in hindered rotation about the C(=O)—O linkage. Since the latter would be infra-red inactive in the planar terephthalate framework (symmetry D_{2h}) its appearance at ~ 70 cm^{-1} in amorphous polymer would confirm the significant lowering of the terephthalate ring symmetry to C_{2v}, in which symmetry the torsion is infra-red active. Its appearance in the spectrum of the oriented crystalline polymer is attributed to the presence of amorphous polymer, known to be present in appreciable proportion in highly crystalline PET[15], and not to lowering of the symmetry of the crystallites. Consequently, a 'doubtlet' is not expected here since ν_{58} is expected to be the infra-red active τ mode of the species B_{2g} of D_{2h} symmetry, and ν'_{58}, $\tau^{\parallel}_{\text{CCOC}}$, is assigned to ~ 70 cm^{-1}.

Weak, broad absorption at ~ 70 cm^{-1} was also observed in ethylene glycol terephthalate and ethylene glycol dibenzoate. Similar absorption at ~ 70 cm^{-1} of σ polarization was observed in PCHT. Such rotations of the terephthalate framework about the chain axis are expected to occur at similar frequencies in both polymers.

ASSIGNMENT OF OVERTONE AND COMBINATION BANDS IN PET

Characteristic combination bands involving the out-of-plane CH bending vibrations are known to give rise to weak infra-red bands in benzene[18] and disubstituted benzene[17] and on this basis a number of bands in PET have been assigned as combination tones[5,6]. The bands at 633, 796, 898, 1 370 and 1 410 cm^{-1}, however, have been shown above to be fundamentals of the PET repeat unit. In a complex spectrum combination bands appearing weakly will be masked by the stronger fundamentals and the weaker (Raman active) fundamentals will be overlapped by the characteristic $\delta_{\text{CH}\perp}$ modes.

The remaining combination and overtone assignments[5] are shown in *Table 6*. Assignments of combination tones have not been attempted for

bands in the region 2 800–2 000 cm^{-1} since many alternative assignments are possible.

CRYSTAL FIELD EFFECTS AND THE EFFECTS OF DRAWING ON THE SPECTRUM OF PET

The results indicate that significant band shifts occur for most of the '*B*' type modes, the extent of the shift depending on the degree of orientation and crystallization of the sample. There is expected to be a minor shift in frequency for a particular vibration due to the difference in molecular configuration between the V_h and C_{2v} symmetry forms. The situation is complicated, however, by the influence in crystalline samples of strong crystal field effects. In oriented films of high crystallinity, spectral changes will arise due to changes in coupling of the crystal field. The very weak bands in PET occurring predominantly in highly oriented heat-crystallized specimens at 3 185, 3 115, 2 725, 2 674, 2 564, 2 457, 2 410, 2 183, 2 079, 1 681, 584, 546, 474 and 458 cm^{-1} probably appear by this effect.

Many bands not only shift in frequency but also change in intensity as a result of drawing PET and the origin of such bands is attributable to rotational isomerism of the glycol residue. Bands affected in this manner include those at 1 448, 1 377, 1 041, 893, 852 and 504 cm^{-1}. In addition, nearly all the bands assigned to the 'internal' skeletal vibrations in *Table 12* are particularly affected by drawing, which is clearly seen in *Figure 2*. In general, those skeletal vibrations having a crystal origin are increased in intensity upon drawing and the intensities of the bands having amorphous origin are diminished. This effect is most probably due to a change in molecular configuration of the glycol residue from a *gauche* configuration in amorphous regions to a *trans* configuration in highly oriented polymer.

The effects of cold-drawing an amorphous PET film on the low-frequency skeletal vibrations are different to those observed in *cis*- and *trans*-PCHT. In PET the bands corresponding to the 'crystal' band components of the *trans*/*gauche* 'doublets' (*Table 12*) intensify and the amorphous components diminish upon drawing and the process is accelerated upon annealing of the sample. In *cis*- and *trans*-PCHT, however, there is little change in intensity of the majority of these 'internal' skeletal modes upon drawing and annealing. The effect is further evidence for the *trans–gauche* isomerism in PET. However, the presence of the 74 cm^{-1} band in *trans*-PCHT, which is of definite crystal origin, is still unexplained.

The frequency shifts and intensity changes brought about by drawing PET are less significant in the case of the terephthalate framework since the change in potential field of the V_h configuration on being lowered to C_{2v} symmetry will almost certainly be less than in the $C_{2h} \rightarrow C_2$ transformation of the ethylene glycol residue.

DISCUSSION

The rigid crystalline model proposed by Bunn *et al.*[11] for PET is not wholly consistent with the spectrum of the highly crystalline polymer. Additional rotation about the —CH_2—O— and —C(=O)—O— bonds occurs to that pre-

dicted in the above model but the space group $P\bar{1}$ of the polymer repeat unit is still conserved. There appears to be more rotational hindrance about the —CH_2—O— and —C(=O)—O— bonds in the crystal than in the amorphous polymer. The presence of the 'doublets' in the submillimetre infra-red spectra of the crystalline and amorphous material are evidence of the presence of the discrete *trans* and *gauche* isomeric configurations of the ethylene glycol fragment, respectively.

The existence of the discrete *trans* and *gauche* configurations of the ethylene glycol residue is further supported by the presence of bands in the conventional and far infra-red regions which are characteristic of crystal and amorphous phases in PET and which are not present in the related polymers *cis*- and *trans*-PCHT. The frequencies of these 'crystal' and 'amorphous' bands agree closely with those predicted for the ethylene glycol residue in PET[23] on the basis of a normal coordinate calculation for the *trans* and *gauche* configurations of the fragment, respectively.

The spectra indicate that the terephthalate framework becomes increasingly distorted with a diminishing crystal field, from a planar conjugated system of D_{2h} symmetry in very highly crystalline polymer to a distorted C_{2v} framework in amorphous regions. Since amorphous polymer still contains a significant proportion of crystallites the 'crystal' bands associated with the *trans* glycol configuration and the planar terephthalate system still appear weakly in the spectra of amorphous PET. These 'crystal' bands disappear, however, in the molten polymer and in the melt of the associated model compounds[8].

Finally, the infra-red spectrum of PET can be successfully interpreted by considering only the local symmetries of the fragments making up the polymer repeat unit. The degree of crystallinity can be correlated with a planar terephthalate framework of D_{2h} symmetry and an ethylene glycol fragment of *trans* configuration of C_{2h} symmetry whilst the amorphous content can be correlated with a non-planar terephthalate skeleton of symmetry of C_{2v} and a *gauche* configuration of the ethylene glycol fragment of C_2 symmetry.

We thank Imperial Chemical Industries Ltd, for the samples of 'Melinex' and Dr A. E. Martin (Sir Howard Grubb Parsons & Co. Ltd) for the provision of experimental facilities. We are indebted to Newcastle upon Tyne Education Committee for the provision of a Research Studentship (to D.A.W.). The work is supported by the Science Research Council.

Department of Chemistry,
Rutherford College of Technology,
Newcastle upon Tyne, NE1 8ST

(*Received August 1968*)

REFERENCES

[1] WARD, I. M. *Chem. & Ind.* **1956,** 905; **1957,** 1102
[2] DANIELS, W. W. and KITSON, R. E. *J. Polym. Sci.* 1958, **33,** 61
[3] GRIME, D. and WARD, I. M. *Trans. Faraday Soc.* 1958, **54,** 959

[4] MIYAKE, A. *J. Polym. Sci.* 1959, **38**, 479
[5] LIANG, C. Y. and KRIMM, S. *J. molec. Spectr.* 1959, **3**, 554
[6] KRIMM, S. *Fortschr. Hochpolym.-Forsch.* 1960, **2**, 153
[7] FARROW, G, MCINTOSH, J. and WARD, I. M. *Makromol. Chem.* 1960, **37**, 147
[8] TADOKORO, H., TATSUKA, K. and MURAHASHI, S. *J. Polym. Sci.* 1962, **59**, 413
[9] MANLEY, T. R. and WILLIAMS, D. A. *Spectrochim. Acta*, 1965, **21**, 737
[10] MANLEY, T. R. and WILLIAMS, D. A. 'Polarized far infra-red spectra of poly-(ethylene terephthalate)'—Paper presented at I.U.P.A.C. Symposium, Brussels, 1967
[11] DAUBENY, R. DE P., BUNN, C. W. and BROWN, C. J. *Proc. Roy. Soc. A*, 1954, **226**, 531
[12] LIANG, C. Y. *J. molec. Spectr.* 1957, **1**, 61
[13] LIANG, C. Y. and KRIMM, S. *J. Polym. Sci.* 1958, **27**, 241
[14] PITZER, K. S. and SCOTT, D. H. *J. Amer. chem. Soc.* 1943, **65**, 803
[15] KOLB, H. J. and IZARD, E. F. *J. appl. Phys.* 1949, **20**, 571
[16] BOYE, C. A. *J. Polym. Sci.* 1961, **55**, 263
[17] WHIFFEN, D. H. *Phil. Trans. A*, 1955, **248**, 131
[18] MAIR, R. D. and HORNIG, D. F. *J. chem. Phys.* 1949, **17**, 1236
[19] GONZALES-SANCHEZ, F. *Spectrochim. Acta*, 1958, **12**, 17
[20] WALTON, W. L. and HUGHES, R. B. *J. Amer. chem. Soc.* 1957, **79**, 3985
[21] HERZFELD, N., HOBDEN, J. W., INGOLD, C. K. and POOLE, H. G. *J. chem. Soc.* **1946**, 272
[22] BAILEY, C. R., CARSON, S. C., GORDON, R. R., and INGOLD, C. K. *J. chem. Soc.* **1946**, 288
[23] BOITSOV, V. G. and GOTLIB, Yu. Ya. *Opt. i Spektr.* 1963, **15** (2), 216
[24] SAWODNY, W., NIEDENZU, K. and DAWSON, J. W. *Spectrochim. Acta*, 1967, **23A**, 799
[25] KANBAYASHI, U. and NAKUDA, K. *Nippon Kagaku Zasshi*, 1963, **84**, 297
[26] BUNN, C. W. *J. Polym. Sci*, 1955, **16**, 323
[27] WILMSHURST, J. K. *J. molec. Spectr.* 1957, **1**, 201
[28] FATELEY, W. G., HARRIS, R. K., MILLER, F. A. and WITKOWSKI, R. E. *Spectrochim. Acta*, 1965, **21**, 231
[29] MILLER, F. A., FATELEY, W. G. and WITKOWSKI, R. E. *Spectrochim. Acta*, 1967, **23A**, 891